Honing Up a Genre of Amphiphilic Bistable [2]Rotaxanes for Device Settings

Jan O. Jeppesen,*[a] Sune Nygaard,[a] Scott A. Vignon,[b] and J. Fraser Stoddart*[b]

Dedicated to Professor Jan Becher on the occasion of his retirement

Keywords: Electrochemistry / Kinetics / Molecular shuttles / Molecular switches / Rotaxanes / Tetrathiafulvalenes

In response to molecular electroactive device requirements, a molecular shuttle in the shape of an amphiphilic bistable [2]rotaxane has been designed, synthesized, and characterized. It contains a hydrophobic, tetraarylmethane and a hydrophilic, dendritic stopper and two π-electron-rich stations—a (monopyrrolo)tetrathiafulvalene unit and a 1,5-dioxynaphthalene moiety — on the rod section of its dumbbell component, which can act as recognition sites for the tetracationic cyclophane, cyclobis(paraquat-*p*-phenylene), to reside around. In contrast to a previously reported "slow" amphiphilic bistable [2]rotaxane, which has an SMe group attached directly to the (monopyrrolo)tetrathiafulvalene unit, this "new and improved" bistable [2]rotaxane has a much less bulky hydrogen atom attached to the (monopyrrolo)tetrathiafulvalene unit. This seemingly small difference in the substituents on the (monopyrrolo)tetrathiafulvalene unit leads to profound changes when comparing the physical properties of the two bistable [2]rotaxanes. Two hydrophilic semidumbbell compounds, comprising only a (monopyrrolo)tetrathiafulvalene unit, and one hydrophobic semidumbbell compound comprising only a 1,5-dioxynaphthalene moiety on its rod section have also been prepared and used to form their corresponding cyclobis(paraquat-*p*-phenylene) complexes. The kinetics of the complexation/decomplexation process occurring in these complexes have been investigated, using both absorption and ^{1}H NMR spectroscopy. In addition, these model complexes have been used to investigate the strength of the noncovalent bonding interactions occurring between the cyclobis(paraquat-*p*-phenylene) ring component and the semidumbbell component at different temperatures, allowing the free energies, enthalpies, and entropies for the formation of these complexes to be determined. The outcome of these investigations can be used to explain the fact that the "slow" [2]rotaxane exists as a 1:1 mixture of its two possible translational isomers, whereas the "new and improved" [2]rotaxane exists as a 4:1 mixture in favor of the translational isomer where the cyclobis(paraquat-*p*-phenylene) tetracation encircles the (monopyrrolo)tetrathiafulvalene unit, and also to explain the thermochromic behavior of the "new and improved" [2]rotaxane. In this amphiphilic bistable [2]rotaxane, shuttling of the cyclobis(paraquat-*p*-phenylene) tetracation can be driven by both chemical and electrochemical oxidation of the (monopyrrolo)tetrathiafulvalene unit rendering it a good candidate for incorporation into two-terminal molecular switch tunnel junctions.

Introduction

The rise of supramolecular chemistry,[1] and its precise dependence on delicate noncovalent bonding interactions, has stimulated research by chemists of many different persuasions in mechanically interlocked compounds like catenanes and rotaxanes.[2] The internal guidance, provided by their intercomponent noncovalent bonds, has transformed these interlocked molecular compounds from chemical curiosities into the centerpieces of a vibrant area of contemporary research in nanochemistry.[3] Since the mechanically-interlocked components of nondegenerate catenanes and rotaxanes can be induced to change their relative positions as a result of some well-chosen external stimulus, they are ideally suited for the construction of artificial molecular machines[3,4,5] and the fabrication of nanoelectronic devices.[6,7,8] Further, because large-amplitude motions can be envisaged[9] within bistable [2]rotaxanes, without the risk of damage to their molecular structures, they can serve as archetypical molecules for the development of nano-electro-mechanical systems (NEMS).

The relative movements, such as circumrotation[10] (rotary motion) and shuttling[11] (linear motion), of the interlocked components can be triggered by chemical, electrochemical, and photochemical stimuli,[12] forcing bistable [2]catenanes and bistable [2]rotaxanes, respectively, to switch between two non-degenerate states (State 0 and State 1). Much effort has been devoted over the past two

[a] Department of Chemistry, Odense University (University of Southern Denmark), Campusvej 55, 5230, Odense M, Denmark
Fax: (internat.) + 45-66-15-87-80
E-mail: joj@chem.sdu.dk
[b] Department of Chemistry and Biochemistry, University of California, Los Angeles, 405 Hilgard Avenue, Los Angeles, CA 90095−1569, USA
Fax: (internat.) + 1-310-206-1843
E-mail: stoddart@chem.ucla.edu

  DOI: 10.1002/ejoc.200400530

decades in trying to understand and control the use of noncovalent bonding interactions in the template-directed synthesis[10,11,13] of such catenanes and rotaxanes. A [2]rotaxane containing two constitutionally different recognition sites (“stations”) in its dumbbell-shaped component can exist in two different nondegenerate co-conformations[14] as translational isomers, whose relative populations reflect their free energy difference as determined primarily by the strengths of the two different sets of noncovalent bonding interactions. In suitably designed bistable [2]rotaxanes, the ring component resides preferentially − in ideal cases[9] only − on one of the two recognition sites. In such systems, the properties of the preferential recognition site can be reversibly altered in response to either physical (light activation) or chemical (redox or pH changes) stimuli.[12] As a consequence, shuttling of the ring component between the two stations can occur.[13] Recently, we reported[15] the template-directed syntheses of amphiphilic bistable [2]rotaxanes in which the ring component is cyclobis(paraquat-*p*-phenylene) ($CBPQT^{4+}$) and the dumbbell component — containing a (monopyrrolo)-TTF (MPTTF) unit and a 1,5-dioxynaphthalene (DNP) moiety within its rod section — is terminated by a hydrophilic dendritic stopper at one end and a hydrophobic tetraarylmethane stopper at the other. These molecules have already been used in the fabrication of solid-state, nanoelectronic devices.[8e] In the case of the [2]rotaxane $\mathbf{1}^{4+}$ (Figure 1), it transpired[15] that the SMe group, situated between the MPTTF and the DNP recognition sites, contributes substantially to a considerable activation barrier for the shuttling of the tetracationic cyclophane $CBPQT^{4+}$ between the two recognition sites, rendering the device performance of this molecule poor. In addition, both absorption and ^1H NMR spectroscopy have demonstrated[15] the presence, in Me_2CO (CD_3COCD_3) solution, of two stable translational isomers in an approximately 1:1 ratio at room temperature. Since the MPTTF recognition site fails to entice the $CBPQT^{4+}$ ring component to reside exclusively on it, its subsequent oxidation, and removal of its stabilizing interactions with the $CBPQT^{4+}$ ring component produces a switch that works in no more than 50% of the [2]rotaxane molecules. By replacing the SMe group on the MPTTF unit in the [2]rotaxane $\mathbf{1}^{4+}$ with the very much less bulky hydrogen atom − producing the [2]rotaxane $\mathbf{2}^{4+}$ (Figure 1) − we expected that the activation barrier for the shuttling of the tetracationic cyclophane $CBPQT^{4+}$ between the MPTTF and the DNP recognition sites will be considerably decreased. In addition, it had also been shown[16] that the binding constant (K_a) increases threefold when the 1:1 complexation of the tetracationic cyclophane $CBPQT^{4+}$ with the MPTTF derivatives **6** (K_a = 1300 M^{-1}, Me_2CO) and **7** (K_a = 3900 M^{-1}, Me_2CO) is compared (Figure 2). Therefore, it was anticipated that the predominant

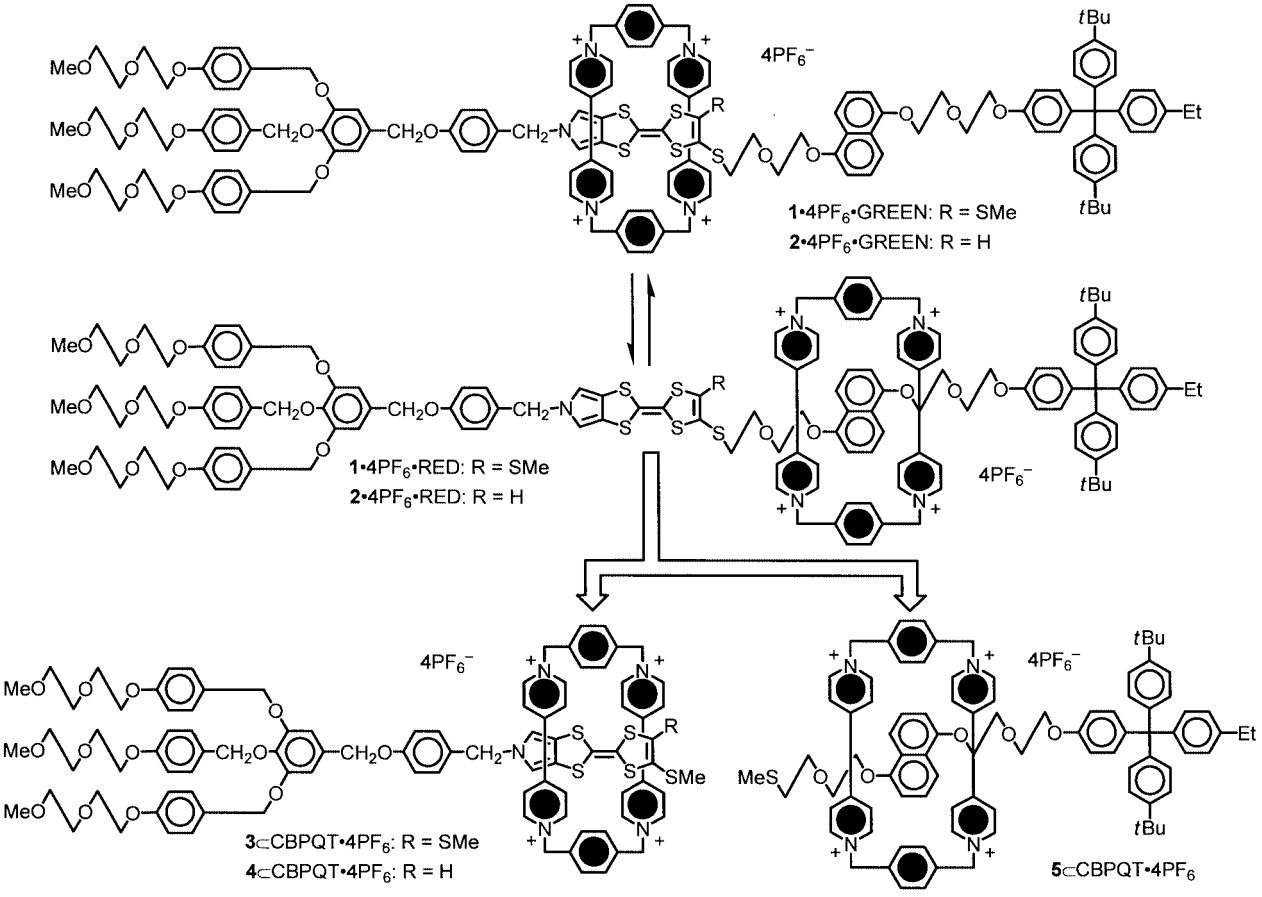

Figure 1. Molecular formulas of the “slow” two-station [2]rotaxane **1**·$4PF_6$, the “fast” two-station [2]rotaxane **2**·$4PF_6$, and some model complexes **3**⊂$CBPQT^{4+}$, **4**⊂$CBPQT^{4+}$, and **5**⊂$CBPQT^{4+}$

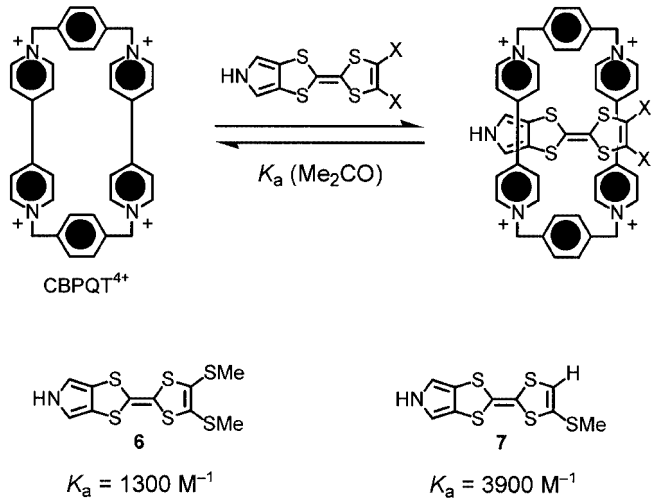

Figure 2. Complexation of the MPTTF derivatives **6** and **7** by $CBPQT^{4+}$

translational isomer of the [2]rotaxane $\mathbf{2}^{4+}$ will be the one in which $CBPQT^{4+}$ encircles the MPTTF unit.

Here, we describe (1) the synthesis of the "new and improved" amphiphilic bistable [2]rotaxane $\mathbf{2}\cdot 4PF_6$, in which the SMe group situated between the MPTTF and DNP recognition sites in the "slow" molecular shuttle/switch $\mathbf{1}\cdot 4PF_6$, has been replaced (Figure 1) by a hydrogen atom. Subsequently, (2) the syntheses of three model compounds − namely two hydrophilic semidumbbell compounds **3** and **4** comprising only an MPTTF unit on their rod sections and a hydrophobic semidumbbell compound **5** comprising only a DNP moiety on its rod section − are described. Thereafter, we compare (3) the photophysical and ^1H NMR spectroscopic properties of the amphiphilic bistable [2]rotaxanes $\mathbf{1}^{4+}$ and $\mathbf{2}^{4+}$, followed by describing (4) thorough kinetic and thermodynamic investigations of their corresponding model complexes $\mathbf{3}\subset CBPQT^{4+}$, $\mathbf{4}\subset CBPQT^{4+}$, and $\mathbf{5}\subset CBPQT^{4+}$. Finally, (5) the chemical redox-switching of $\mathbf{2}^{4+}$, together with (6) some electrochemical studies performed on $\mathbf{2}^{4+}$ and on the model complexes $\mathbf{3}\subset CBPQT^{4+}$, $\mathbf{4}\subset CBPQT^{4+}$, and $\mathbf{5}\subset CBPQT^{4+}$ are discussed.

Results and Discussion

Synthesis

The syntheses (Scheme 1) of the DNP moiety[15] **11** carrying the hydrophobic stopper and the chloride **15** carrying the hydrophilic stopper,[8b,17] have already been reported. Here, we describe the syntheses (Schemes 1 and 2) of a novel MPTTF building block **10** and the "fast" molecular shuttle/switch $\mathbf{2}\cdot 4PF_6$, before outlining (Schemes 3−5) the syntheses of the two hydrophilic semidumbbell compounds **3** and **4** and the hydrophobic semidumbbell compound **5**.

The synthesis of the asymmetric MPTTF building block **10** was carried out as outlined in Scheme 1. Cross-coupling of 5-tosyl-5*H*-1,3-dithiolo[4,5-*c*]pyrrol-2-one[18] (**8**) with

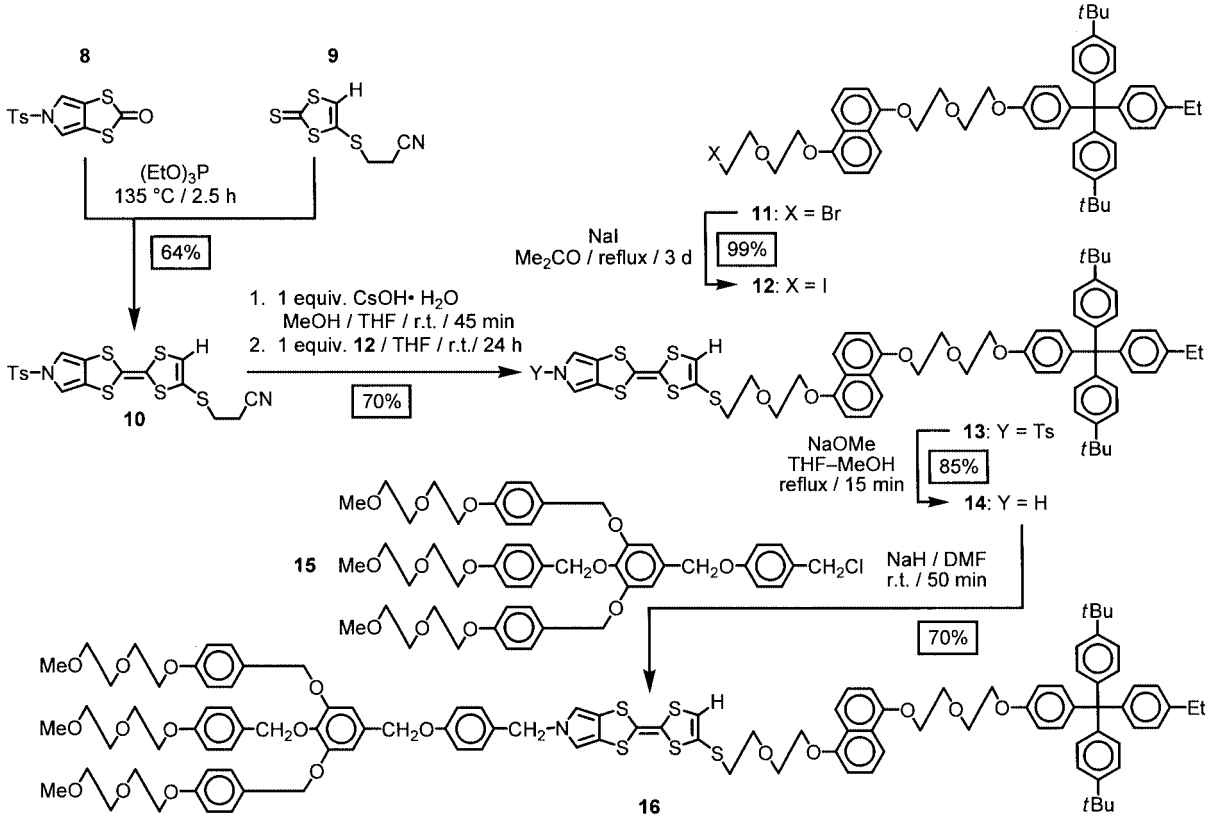

Scheme 1. Synthesis of the dumbbell compound **16**

two equivalents of 4-(2-cyanoethylthio)-1,3-dithiole-2-thione[19] (**9**) in neat $(EtO)_3P$ gave **10** in 64% yield. The dumbbell compound **16**, the precursor to the "fast" molecular shuttle/switch **2**·4PF_6, was synthesized as illustrated in Scheme 1. Treatment of the bromide[15] **11** with NaI gave, in almost quantitative yield, the iodide **12**, which could be coupled with the MPTTF building block **10** following its in situ deprotection with one equivalent of $CsOH·H_2O$ to give **13** in 70% yield. The tosyl protecting group on the MPTTF unit was removed in good yield (85%) by using NaOMe in a THF/MeOH mixture. The resultant pyrrole nitrogen atom in **14** was alkylated with the chloride[8b,17] **15**, and the dumbbell compound **16** was isolated in 70% yield. The [2]rotaxane **2**·4PF_6 was self-assembled (Scheme 2) under high pressure conditions[20] by using the dumbbell compound **16** as the template for the formation of the encircling $CBPQT^{4+}$ tetracation, and the [2]rotaxane **2**·4PF_6 was isolated in 55% yield from a mixture of the dumbbell compound **16**, the dicationic precursor[10] **17**·2PF_6, and the dibromide **18** after they had been subjected to a 10 kbar pressure in DMF at room temperature for 3 days.

The semidumbbell compounds **3**−**5** were synthesized as shown in Schemes 3−5. *N*-Alkylation of the MPTTF derivative[18] **6** with the chloride[8b,17] **15** gave (Scheme 3) the hydrophilic semidumbbell compound **3** in 81% yield. In order to construct the hydrophilic semidumbbell compound **4**, the MPTTF building block **10** was treated (Scheme 4) with one equivalent of $CsOH·H_2O$. This procedure generated the MPTTF-monothiolate, which was alkylated with MeI, to give the MPTTF derivative **19** in almost quantitative yield. Removal of the tosyl protecting group was carried out in 88% yield using NaOMe in a THF/MeOH mixture. Finally, the hydrophilic semidumbbell compound **4** was obtained in 71% yield, following *N*-alkylation of the pyrrole unit in **7** with the chloride[8b,17] **15**. Treatment of the iodide **12** with NaSMe afforded (Scheme 5) the hydrophobic semidumbbell compound **5** in excellent yield (99%).

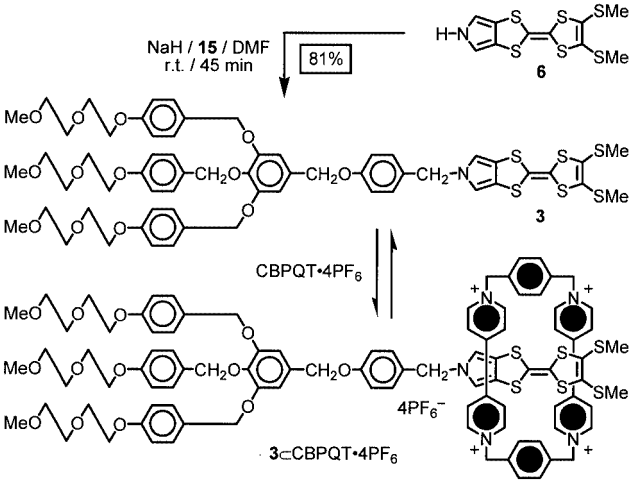

Scheme 3. Synthesis of the semidumbbell compound **3** and its complexation by CBPQT·4PF_6

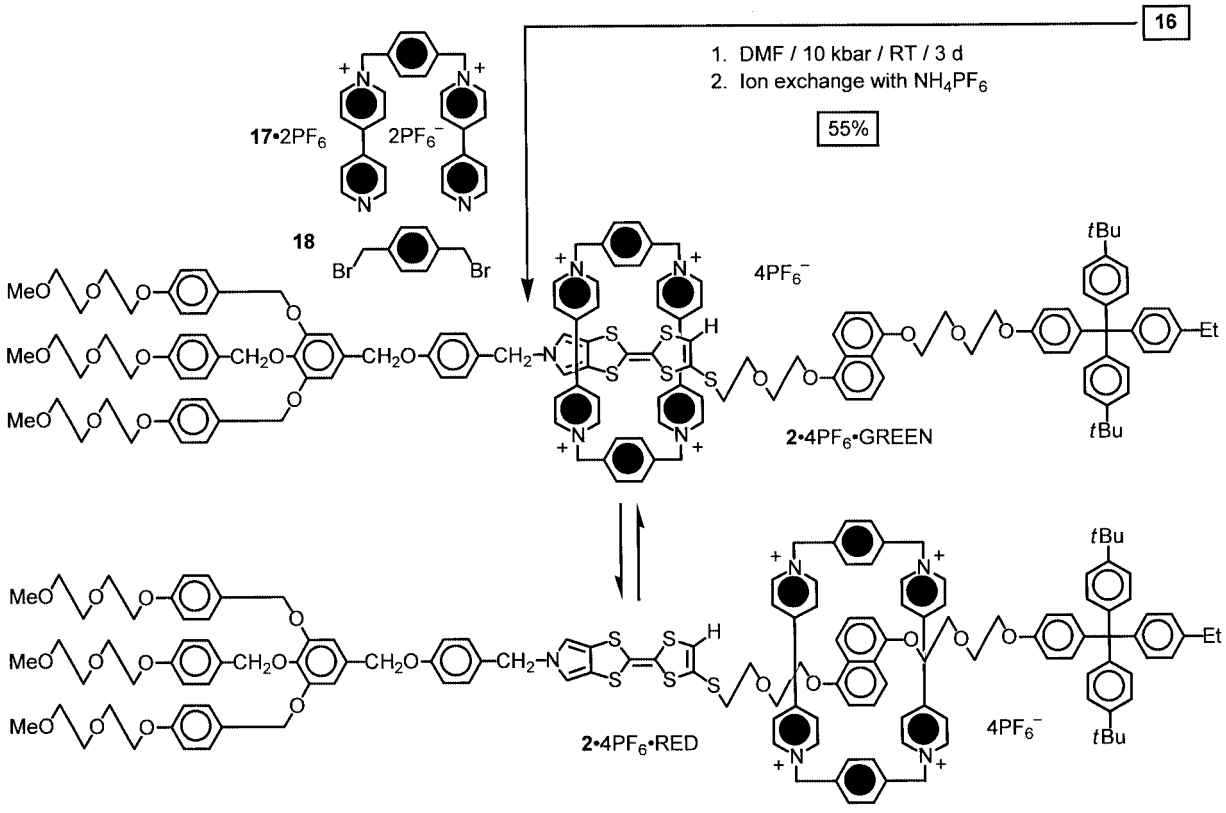

Scheme 2. Synthesis of the "fast" two-station [2]rotaxane **2**·4PF_6

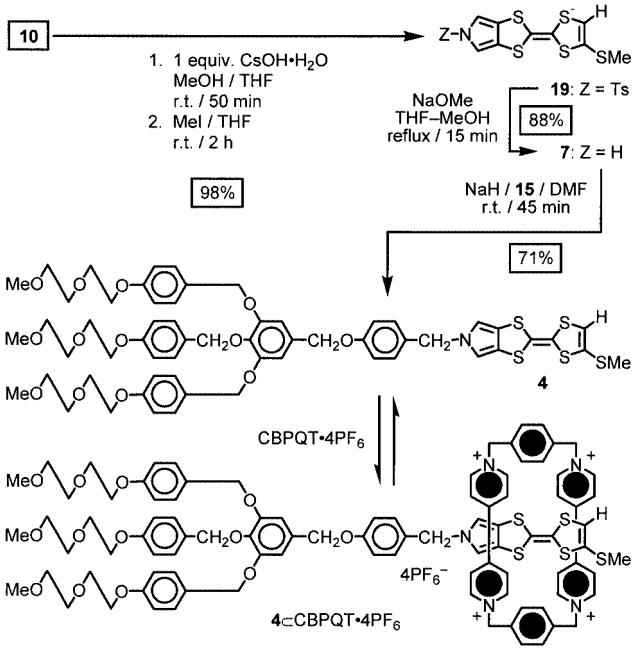

Scheme 4. Synthesis of the semidumbbell compound **4** and its complexation by CBPQT·4PF$_6$

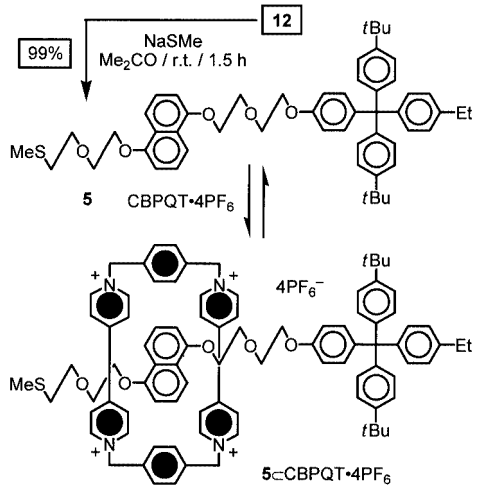

Scheme 5. Synthesis of the semidumbbell compound **5** and its complexation by CBPQT·4PF$_6$

Mass Spectrometric Investigations

The dumbbell compound **16**, the semidumbbell compounds **3**−**5**, and the [2]rotaxane **2**·4PF$_6$ were all characterized by matrix-assisted laser-desorption/ionization time-of-flight (MALDI-TOF) mass spectrometry. The spectra obtained for **3**−**5** and **16** gave peaks corresponding to the $[M]^+$ ion, whereas the spectrum for **2**·4PF$_6$ gave peaks corresponding to the $[M - 3PF_6]^+$ and $[M - 4PF_6]^+$ ions.

Photophysical Investigations

Just as observed[15b] previously for the dumbbell component of the [2]rotaxane $\mathbf{1}^{4+}$, the absorption spectrum of the dumbbell compound **16** is quite similar to the sum of the spectra of its chromophoric units, indicating that, in dumbbell compound **16**, there are no significant interactions among its chromophoric units in the ground state.

In contrast to the [2]rotaxane **1**·4PF$_6$ which was isolated as a brown solid, the [2]rotaxane **2**·4PF$_6$ was isolated as a dark green solid. This observation indicates that the major translational isomer of $\mathbf{2}^{4+}$ is **2**·GREEN^{4+}. The absorption spectrum (Figure 3), recorded from $\mathbf{2}^{4+}$ in Me_2CO at 298 K, reveals a broad charge transfer (CT) absorption band centered at 815 nm (ε = 1410 L·mol^{-1}·cm^{-1}), which is characteristic[21] of co-conformations containing an MPTTF unit located inside CBPQT^{4+}. This band is accompanied by a CT absorption band − observed as a tiny shoulder at 520 nm (ε = 850 L·mol^{-1}·cm^{-1}) − which results from the DNP moiety that is located inside the CBPQT^{4+} ring.[22] A comparison of the absorption spectra (Figure 3) of equilibrium mixtures of the [2]rotaxanes $\mathbf{1}^{4+}$ and $\mathbf{2}^{4+}$ recorded in Me_2CO at 298 K indicates clearly that the translational isomer in which CBPQT^{4+} encircles the MPTTF is more populated in the case of $\mathbf{2}^{4+}$, since the MPTTF/CBPQT^{4+} CT interaction, centered around 800 nm, for $\mathbf{2}^{4+}$ is significantly stronger than that observed for $\mathbf{1}^{4+}$.

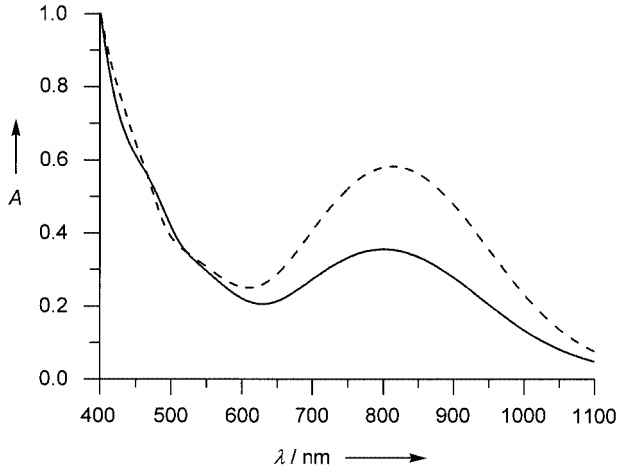

Figure 3. Absorption spectra recorded at 298 K in Me_2CO of equilibrium mixtures of the [2]rotaxanes **1**·GREEN^{4+} and **1**·RED^{4+} (——) and of the [2]rotaxanes **2**·GREEN^{4+} and **2**·RED^{4+} (− −); both spectra were recorded using 0.41 mM solutions of $\mathbf{1}^{4+}$ and $\mathbf{2}^{4+}$, respectively

We have previously reported[15] that the two-station [2]rotaxane $\mathbf{1}^{4+}$ was isolated as a 1:1 mixture of **1**·GREEN^{4+} and **1**·RED^{4+}. It was found[15] that the absorption spectrum of the isolated 1:1 mixture of the two-station [2]rotaxane $\mathbf{1}^{4+}$ recorded in MeCN at 298 K changes with time, such that the absorption bands for the MPTTF/CBPQT^{4+} CT interaction — centered around 820 nm — increases in intensity and the DNP/CBPQT^{4+} CT interaction — centered around 520 nm — decreases in intensity, indicating clearly that shuttling of CBPQT^{4+} from the DNP recognition site in **1**·RED^{4+} to the MPTTF recognition site occurs. After 20 h under these conditions, the system reaches equilibrium, and no perceptible changes are observed in ab-

sorption spectra recorded subsequently. ^{1}H NMR spectroscopy reveals[15b] that the equilibrated MeCN (CD_3CN) solution contained a 3:1 mixture of **1**·GREEN^{4+} and **1**·RED^{4+}. In the case of the two-station [2]rotaxane **2**$^{4+}$, equilibration occurs much more rapidly and the absorption spectrum (Figure 4) of **2**$^{4+}$ recorded in MeCN at 298 K does not change with time. A comparison of the absorption spectra (Figure 4) recorded in MeCN at 298 K of equilibrium mixtures of the [2]rotaxanes **1**$^{4+}$ and **2**$^{4+}$ indicates clearly that the translational isomer in which CBPQT^{4+} encircles the MPTTF is more populated in the case of **2**$^{4+}$.

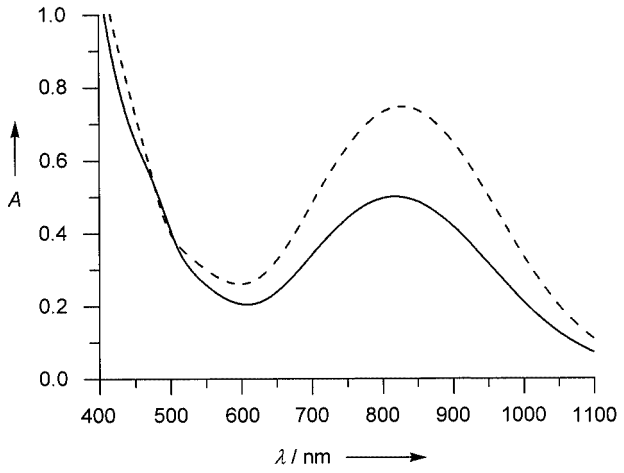

Figure 4. Absorption spectra recorded at 298 K in MeCN of equilibrium mixtures of the [2]rotaxanes **1**·GREEN^{4+} and **1**·RED^{4+} (——) and of the [2]rotaxanes **2**·GREEN^{4+} and **2**·RED^{4+} (– –); both spectra were recorded using 0.41 mM solutions of **1**$^{4+}$ and **2**$^{4+}$, respectively; in the [2]rotaxane **2**$^{4+}$, equilibration occurs immediately; however, in the case of the slow [2]rotaxane **1**$^{4+}$, equilibration takes 24 h

Figure 5 shows the absorption spectra of the [2]rotaxane **2**$^{4+}$ recorded in MeCN, Me_2CO, and Me_2SO. In all these solvents, a broad absorption band (Table 1) is observed in the region 600−1100 nm, which can be assigned to the CT interactions of the MPTTF unit encircled by CBPQT^{4+}. However, it should be noted that the MPTTF/CBPQT^{4+} CT band decreases significantly in intensity when changing the solvent from MeCN → Me_2CO → Me_2SO, while the DNP/CBPQT^{4+} CT band, at the same time, exhibits a more or less constant intensity, indicating that the solvent has a pronounced influence on the distribution of CBPQT^{4+} between the two stations. These results can be explained by the relative positioning of the MPTTF unit and the DNP moiety with respect to the hydrophilic dendritic stopper. In the [2]rotaxane **2**$^{4+}$, the hydrophilic dendritic stopper is located closer to the MPTTF station and both the CT and [C−H···O] hydrogen-bonding interactions between the hydrophilic stopper and CBPQT^{4+} play an important role as far as the relative occupation of the MPTTF station by CBPQT^{4+} is concerned. When changing the solvent from MeCN → Me_2CO → Me_2SO, the [C−H···O] hydrogen-bonding interactions between the bismethyleneoxy groups of the hydrophilic stopper and some of the α-CH hydrogen atoms in the bipyridinum units of the CBPQT^{4+} ring component[23] become less dominant as a result of competing [C−H···O] hydrogen-bonding interactions that occur between the solvent and CBPQT^{4+}.

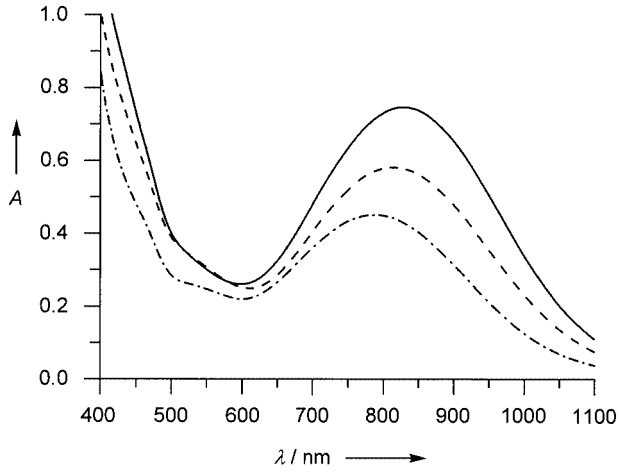

Figure 5. Absorption spectra (298 K) of an equilibrium mixture of the [2]rotaxanes **2**·GREEN^{4+} and **2**·RED^{4+} recorded in MeCN (——), Me_2CO (– –), and Me_2SO (–·–·–); all spectra were recorded using 0.41 mM solutions of **2**$^{4+}$

Table 1. Comparison of the photophysical data[a] at 298 K for the [2]rotaxanes **1**$^{4+}$ and **2**$^{4+}$

		GREEN		RED	
Compound	Solvent	$\lambda_{max.}$ [nm]	ε [L·mol^{-1}·cm^{-1}]	λ[b] [nm]	ε [L·mol^{-1}·cm^{-1}]
1^{4+}	MeCN	820	1220	520	790
1^{4+}	Me_2CO	805	860	520	860
2^{4+}	MeCN	825	1820	520	850
2^{4+}	Me_2CO	815	1410	520	850
2^{4+}	Me_2SO	790	1090	520	640

[a] Data obtained from equilibrated solutions of the two compounds. In the [2]rotaxane **2**$^{4+}$ equilibration occurs immediately. However, in the case of the [2]rotaxane **1**$^{4+}$, equilibrium is reached in approximately 24 h. [b] Observed as a shoulder.

In order to assess the thermochromic properties of the bistable [2]rotaxane **2**$^{4+}$, a temperature-controlled UV/Vis experiment (Figure 6) was carried out in Me_2CO. At 298 K, the absorption bands for both the MPTTF/CBPQT^{4+} CT interaction — centered around 815 nm — and the DNP/CBPQT^{4+} CT interaction — centered around 520 nm — were clearly evident (Figure 6). On increasing the temperature, the CT band, centered around 815 nm, increases in intensity, and the band around 520 nm decreases in intensity. The reverse trend was observed on decreasing the temperature. As a consequence of these spectroscopic variations, the color of the solution changes from greenish brown (low temperature) to pale green (high temperature). This sequence of events indicates that a interconversion of **2**·RED^{4+} into **2**·GREEN^{4+} take place when the tempera-

ture is raised from 288 K to 328 K and that **2**·GREEN^{4+} is the dominant translational isomer at 328 K.

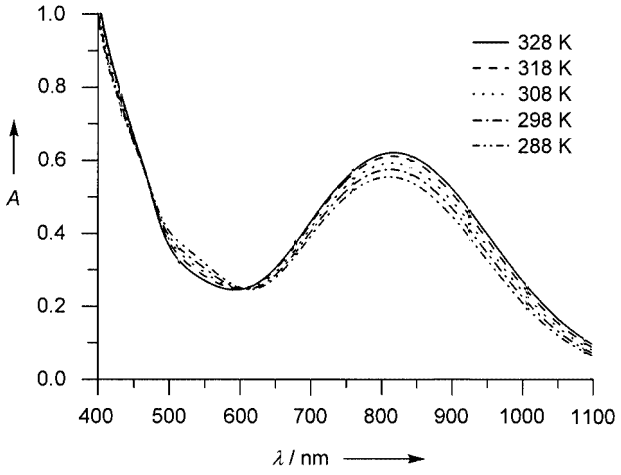

Figure 6. Absorption spectra recorded on an equilibrium mixtures of the [2]rotaxanes **2**·GREEN^{4+} and **2**·RED^{4+} in Me_2CO (0.41 mM) at different temperatures

^{1}H NMR Investigations

While absorption spectroscopy indicates qualitatively the locations of CBPQT^{4+} between the recognition sites on the rod section of the semidumbbell component, ^{1}H NMR spectroscopy provides a quantitative tool for monitoring its precise distribution between the sites and also yields fine, as well as gross, structural information.

Two-Station [2]Rotaxane 2^{4+}

A variable-temperature (VT) ^{1}H NMR investigation of the [2]rotaxane **2**$^{4+}$ was undertaken in order to study the temperature dependence of the equilibrium between the translational isomers **2**·GREEN^{4+} and **2**·RED^{4+}. Three different solvents were used for this investigation, namely, CD_3COCD_3, CD_3CN, and CD_3SOCD_3. Data for the equilibrium distribution of the two translational isomers were obtained at temperatures where the shuttling process is slow on the ^{1}H NMR timescale. Because of the relatively high freezing point for CD_3SOCD_3, determination of the distribution of translational isomers was precluded by the fact that the shuttling process is fast on the ^{1}H NMR timescale at all temperatures above the freezing point. Integration and partial line-shape analysis of the signals arising from the ethyl group on the hydrophobic stopper were used to determine the relative amounts of **2**·GREEN^{4+} and **2**·RED^{4+} present at a given temperature in both CD_3COCD_3 (Figure 7) and CD_3CN (Figure 8), and the results are listed in Table 2 and 3.

A plot showing a summary of the data collected is given in Figure 9. A comparison of the equilibrium at 263 K shows that in CD_3COCD_3 approximately 60% of **2**·RED^{4+} is present with 40% of **2**·GREEN^{4+}. In CD_3CN, the preference is reversed and only 30% of **2**·RED^{4+} is present at 263 K with 70% of the [2]rotaxane existing as **2**·GREEN^{4+}. As can be seen from the plot in Figure 9, the CD_3CN solution shows a markedly larger temperature dependence for this equilibrium relative to the CD_3COCD_3 solution.

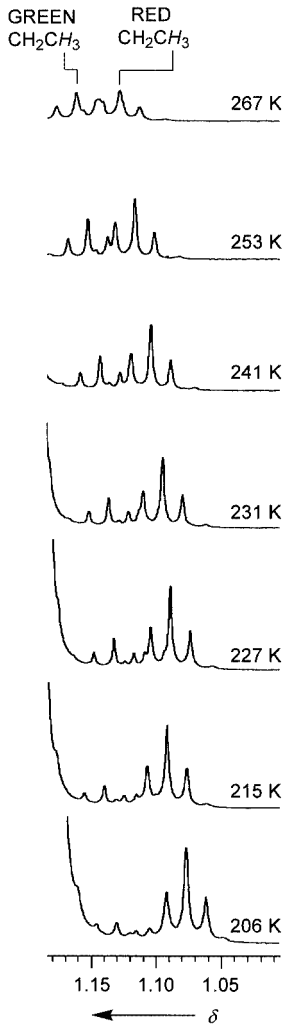

Figure 7. Partial ^{1}H NMR spectra of [2]rotaxane **2**$^{4+}$ recorded in CD_3COCD_3 between 206−267 K showing the signal corresponding to the Me group in the ethyl substituent on the hydrophobic stopper

Table 2. Ratio[a] (K_{eq}) and derived free energies[b] ($\Delta\Delta G$) between the translational isomers **2**·GREEN^{4+} and **2**·RED^{4+} in an equilibrium mixture of the [2]rotaxane **2**$^{4+}$ determined by ^{1}H NMR spectroscopy at different temperatures (T) in CD_3COCD_3

T [K]	K_{eq}[a]	$\Delta\Delta G$[b]
206	0.11	0.90
215	0.22	0.65
227	0.33	0.50
231	0.43	0.39
241	0.59	0.25
253	0.74	0.15
267	0.92	0.04

[a] The ratio K_{eq} = [**2**·GREEN^{4+}]/[**2**·RED^{4+}] between the translational isomers **2**·GREEN^{4+} and **2**·RED^{4+} was determined by integration and partial line-shape analysis of the signal arising from the CH_3 group in the ethyl substituent on the hydrophobic stopper. [b] $\Delta\Delta G = \Delta G$(**2**·GREEN^{4+}) − ΔG(**2**·RED^{4+}).

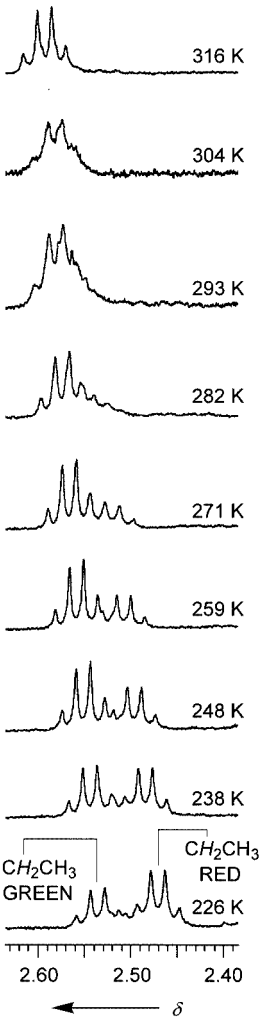

Figure 8. Partial ^{1}H NMR spectra of [2]rotaxane $\mathbf{2}^{4+}$ recorded in CD_3CN between 226−316 K showing the signal corresponding to the CH_2 group in the ethyl substituent on the hydrophobic stopper

Table 3. Ratio[a] (K_{eq}) and derived free energies[b] ($\Delta\Delta G$) between the translational isomers **2**·GREEN^{4+} and **2**·RED^{4+} in an equilibrium mixture of the [2]rotaxanes $\mathbf{2}^{4+}$ determined by ^{1}H NMR spectroscopy at different temperatures (T) in CD_3CN

T [K]	K_{eq}[a]	$\Delta\Delta G$[b]
226	0.67	0.18
238	1.1	−0.04
248	1.6	−0.24
259	2.3	−0.44

[a] The ratio K_{eq} = [**2**·GREEN^{4+}]/[**2**·RED^{4+}] between the translational isomers **2**·GREEN^{4+} and **2**·RED^{4+} was determined by integration and partial line-shape analysis of the signal arising from the CH_2 group in the ethyl substituent on the hydrophobic stopper. [b] $\Delta\Delta G = \Delta G$(**2**·GREEN^{4+}) − ΔG(**2**·RED^{4+}).

Kinetic Investigations

A fundamental understanding of the shuttling behavior in solution by bistable [2]rotaxanes must be achieved if their switching properties in solid-state devices[8] are going to be harnessed to the full. Toward this end, detailed kinetic investigations of the complexation/decomplexation processes for the 1:1 complexes formed between the model semidumbbell compounds **3**−**5** and CBPQT^{4+} were carried out in Me_2CO with the objective of obtaining the kinetic and thermodynamic parameters for the processes.

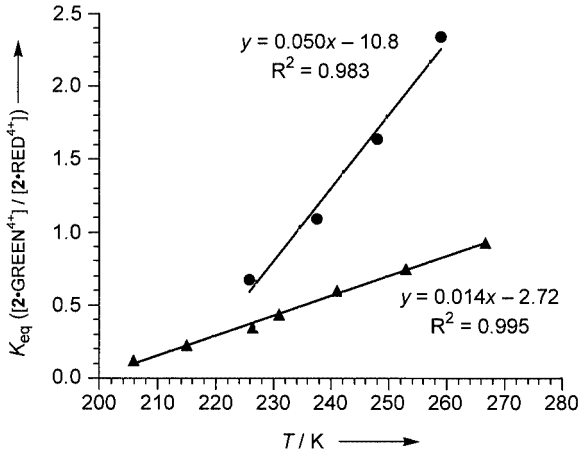

Figure 9. A linear plot of K_{eq} against T for the translational isomerism of the [2]rotaxane $\mathbf{2}^{4+}$ between the **2**·GREEN^{4+} and **2**·RED^{4+} isomers, data in Me_2CO are represented by triangles and MeCN by circles; the K_{eq} values were obtained as described in Table 2 and 3

Two-Station [2]Rotaxane 2^{4+}

The barrier for shuttling of the CBPQT^{4+} ring in $\mathbf{2}^{4+}$ can be determined by observing the coalescence (Figure 7 and 8) of the ^{1}H NMR signals arising from **2**·RED^{4+} and **2**·GREEN^{4+} as the temperature is increased. The rate constant for the shuttling process, k_S, is given by the equation $k_S = (\pi\Delta\upsilon_{ex})/(\sqrt{2})$, where $\Delta\upsilon_{ex}$ is the separation between the peaks at low temperature in Hz. The $\Delta G_c^{\ddagger}$ value can then be calculated, and was determined to be 14.8 kcal·mol^{-1} in CD_3COCD_3 at 293 K and 14.7 kcal·mol^{-1} in CD_3CN at 293 K.

3⊂CBPQT^{4+}

Mixing equimolar amounts (0.89 mM) of the yellow semidumbbell compound **3** and the colorless CBPQT^{4+} ring component[24] in Me_2CO at 297 K produced a yellow solution which slowly became green, an observation that is related to the slow formation (Scheme 3) of the [2]pseudorotaxane **3**⊂CBPQT^{4+}. The process whereby CBPQT^{4+} threads onto the MPTTF unit in **3** could be followed (Figure 10) by monitoring the increase in the intensity of the MPTTF/CBPQT^{4+} CT absorption band centered at 807 nm. After 45 min at 297 K, the system reached equilibrium and no perceptible changes were observed in absorption spectra recorded subsequently. The kinetics of the threading of CBPQT^{4+} onto the MPTTF unit are expected to be first-order.[25] The process whereby CBPQT^{4+} threads onto the semidumbbell compound **3** was investigated using absorption spectroscopy by monitoring the increase in the CT band intensity resulting from the MPTTF unit being

located inside $CBPQT^{4+}$. Immediately after mixing equimolar amounts of $CBPQT^{4+}$ and the semidumbbell compound **3** in Me_2CO,[26] the threading process was followed at different temperatures (Table 4) using the absorbance A at 807 nm as the probe. The experimental data were subjected to a first-order analysis and rate constants (k) were obtained for the threading of $CBPQT^{4+}$ onto the semidumbbell compound **3** at different temperatures. The straight lines obtained (Figure 11) by plotting ln A against time (t) confirmed[27] the first-order nature of the threading process. The k values and the corresponding free energies of activation[28] ($\Delta G^{\ddagger}$) were obtained directly from the slopes of these straight lines and are recorded in Table 4, together with the half-lives ($t_{1/2}$). As expected, the exchange between the complexed and uncomplexed species in the 1:1 complex formed between the semidumbbell compound **3** and $CBPQT^{4+}$ occurs slowly on the ^1H NMR timescale (CD_3COCD_3, 300 MHz) at 300 K.

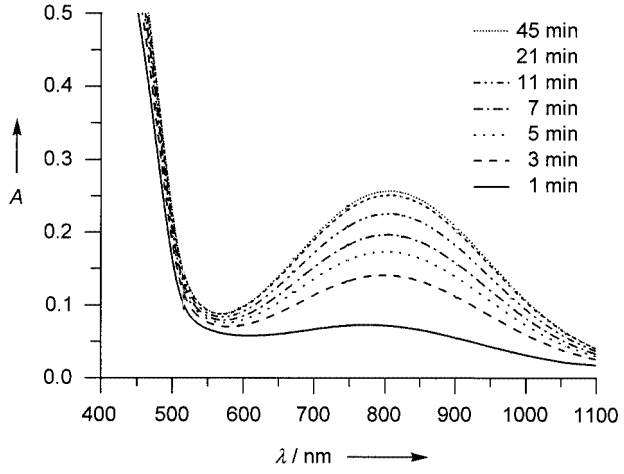

Figure 10. Absorption spectra recorded in Me_2CO at 297 K on a 1:1 mixture of the semidumbbell compound **3** and $CBPQT^{4+}$ at different times after mixing

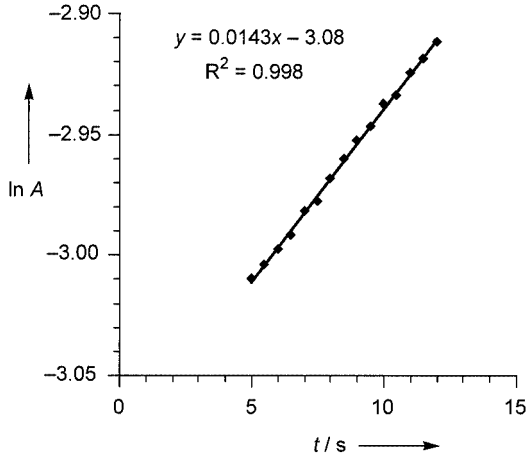

Figure 11. A linear plot of ln A against t for a 1:1 mixture of $CBPQT^{4+}$ and the semidumbbell compound **3** in Me_2CO obtained by using the MPTTF/$CBPQT^{4+}$ CT absorption band (807 nm) as the probe; the absorbance A was measured at 291 K on an initial 0.93 mM solution with respect to both $CBPQT^{4+}$ and **3**; the 15 data points were collected in the early stages of the experiment where the reverse process is not yet occurring to any significant extent; they have been fitted by a best straight line, giving a correlation coefficient of 0.998, indicating that first-order kinetics are in operation

Table 4. Rate constants (k) and derived free energies of activation[28] ($\Delta G^{\ddagger}$) for the threading of $CBPQT^{4+}$ on the semidumbbell compound **3**, determined by absorption spectroscopy in Me_2CO[a] at different temperatures using the MPTTF/$CBPQT^{4+}$ CT band as the probe

T [K]	$\lambda_{max.}$ [nm]	Data Points	Correlation Coefficient	k [s^{-1}]	$t_{1/2}$ [s][b]	$\Delta G^{\ddagger}$ [kcal·mol^{-1}]
287	807	17	0.997	1.25×10^{-2}	55	19.3
290	807	17	0.996	1.37×10^{-2}	51	19.4
291	807	15	0.998	1.43×10^{-2}	48	19.4
292	807	9	0.994	1.47×10^{-2}	47	19.5
293	807	9	0.998	1.66×10^{-2}	42	19.5
296	807	18	0.999	1.94×10^{-2}	36	19.6
297	807	11	0.995	2.01×10^{-2}	34	19.7
299	807	14	0.995	2.04×10^{-2}	34	19.8
301	807	13	0.985	2.30×10^{-2}	30	19.9
303	807	9	0.994	2.54×10^{-2}	27	20.0

[a] Experiments were performed with an initial concentration of the semidumbbell compound **3** (equal to that of $CBPQT^{4+}$) of 0.71 mM.[26] The k values were obtained from the slope of the straight line in the plot of ln A against t using the relationship of $\ln A/A_0 = k\,t + \ln A_0$. The values A and A_0 correspond to the absorbance (at 807 nm) at time t, and to the initial absorbance (at 807 nm), respectively. [b] The values for the "half-life" were obtained from $t_{1/2} = \ln 2/k$ and are the theoretical ones that would be observed in a nonequilibrating system, i.e. if the reverse process was prevented by constant removal of the separated components from the system.

4⊂CBPQT^{4+}

Mixing equimolar proportions (0.75 mM) of the semidumbbell compound **4** and $CBPQT^{4+}$ in Me_2CO leads to the immediate formation (Scheme 4) of the [2]pseudorotaxane **4**⊂$CBPQT^{4+}$, as evidenced by the spontaneous production of a green-colored solution. These results indicate that the threading process leading to the formation of **4**⊂$CBPQT^{4+}$ is a much faster one than the threading process leading to the formation of **3**⊂$CBPQT^{4+}$. In contrast to **3**⊂$CBPQT^{4+}$, the exchange between the complexed and uncomplexed species in a 1:1 mixture of the semidumbbell compound **4** and $CBPQT^{4+}$ occurs rapidly on the ^1H NMR timescale (CD_3COCD_3, 500 MHz) at 303 K. At 196 K, the kinetics enter the regime of slow exchange on the ^1H NMR timescale, and both complexed and uncomplexed species can be observed in the ^1H NMR spectrum (CD_3COCD_3, 500 MHz) recorded on the semidumbbell compound **4** and 0.5 equivalents of $CBPQT^{4+}$.

In order to determine an activation barrier for the complexation/decomplexation process occurring in **4**⊂$CBPQT^{4+}$, a CD_3COCD_3 solution of the semidumbbell compound **4** containing 0.5 equivalents of $CBPQT^{4+}$ was studied using VT ^1H NMR spectroscopy. At 260 K, the spectrum (500 MHz) obtained (Figure 12, a) displays the

expected time-averaged signal for the resonances associated with the protons on the SMe groups. Upon cooling the sample down, a gradual broadening of this signal occurs, which leads eventually, on further cooling, to a separation (Figure 12, e) of this signal into two resonances, which can be associated with the SMe protons in the complexed and uncomplexed forms of the semidumbbell compound **4**. At the coalescence temperature, the activation barrier ($\Delta G_c^{\ddagger}$) for the process whereby a $CBPQT^{4+}$ ring exchanges between two semidumbbell molecules can be calculated[29] and was determined to be 11.7 ± 0.1 kcal·mol^{-1} at 238 K.

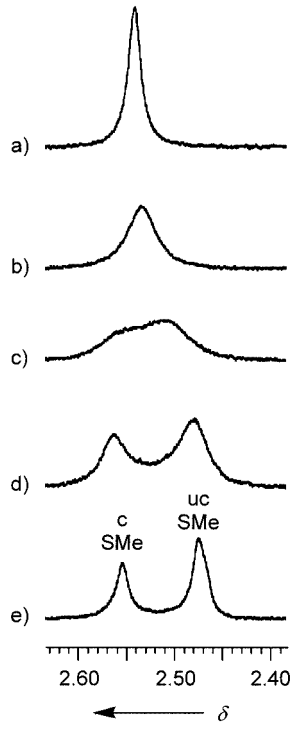

Figure 12. Partial ^{1}H NMR spectra (500 MHz) of the SMe region recorded on a CD_3COCD_3 solution of **4** (1 mM) +0.50 equiv. $CBPQT^{4+}$ at a) 260 K, b) 249 K, c) 238 K, d) 226 K, and e) 215 K; at lower temperatures two signals can be observed for the protons of the SMe group (e); these signals can be attributed to the complexed and uncomplexed forms of **4**; upon increasing the temperature they are observed to broaden (d), coalesce (c), and eventually appear as one signal (b) at 249 K; the descriptions c and uc refer to complexed and uncomplexed species, respectively

5⊂CBPQT^{4+}

Just as in the case of the pseudorotaxane **4**⊂$CBPQT^{4+}$, the exchange between the complexed and uncomplexed species in a mixture of the semidumbbell compound **5** and 0.70 equivalents of $CBPQT^{4+}$ occurs rapidly on the ^{1}H NMR timescale (CD_3COCD_3, 500 MHz) at 303 K (Figure 13, a). At 196 K (Figure 13, b), the kinetics enter the regime of slow exchange on the ^{1}H NMR timescale, and both complexed and uncomplexed species can be observed in the ^{1}H NMR spectrum (CD_3COCD_3, 500 MHz) recorded on the semidumbbell compound **5** and 0.7 equivalents of $CBPQT^{4+}$. In the ^{1}H NMR spectrum (CD_3COCD_3, 500 MHz) recorded (Figure 14, a) at 196 K on a mixture of the semidumbbell compound **5** and a slight excess of $CBPQT^{4+}$, virtually no uncomplexed semidumbbell **5** is present, indicating that the complexation of **5** by $CBPQT^{4+}$ is very strong at this temperature. Evidence for the fact that $CBPQT^{4+}$ encircles the DNP moiety is apparent from the observation of a high upfield shift of the peaks corresponding to the protons of the DNP moiety. As a consequence of the asymmetry present in the semidumbbell component, the DNP-*H*-2/6 protons resonate as two overlapping doublets (J = 8 Hz) at δ = 6.38 ppm, while the DNP-*H*-3/7 protons resonate as two triplets (J = 8 Hz) centered at δ = 6.21 and 6.24 ppm, in the spectrum (Figure 14, a) of **5**⊂$CBPQT^{4+}$. The upfield shift of the DNP-*H*-2/6 and DNP-*H*-3/7 protons results from anisotropic shielding of the protons on the DNP moiety by the aromatic units present in the encircling $CBPQT^{4+}$ ring. Additionally, the DNP-*H*-4/8 protons of the encircled DNP moiety participate in [C−H···π] interactions. The fact that they are pointing toward the π-faces of the *p*-xylylene units of the tetracationic cyclophane $CBPQT^{4+}$ results in a very large upfield shift of their resonances, which are observed as two doublets (J = 8 Hz) at δ = 2.63 and 2.65. The δ values for the DNP-*H*-4/8 protons in **5**⊂$CBPQT^{4+}$ and the same protons in the semidumbbell compound **5** are shifted upfield by 5.24 and 5.22 ppm. Examination of the ^{1}H DQF-COSY (***D***ouble ***Q***uantum ***F***iltered − ***Co***rrelation ***S***pectroscop***y***) spectrum (Figure 14, b) for **5**⊂$CBPQT^{4+}$ clearly shows the scalar coupling between the protons in the DNP moiety.

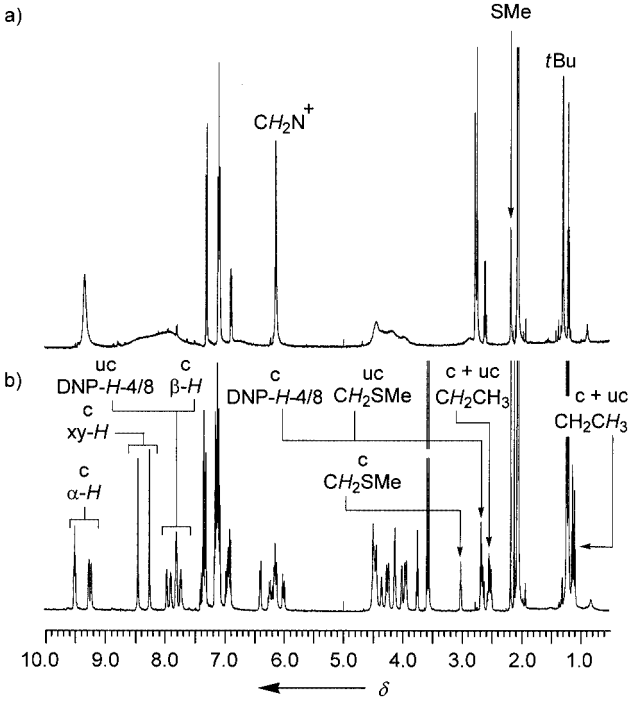

Figure 13. ^{1}H NMR spectra (500 MHz) recorded in CD_3COCD_3 of **5** (1 mM) and 0.7 equivalents $CBPQT^{4+}$ at a) at 303 K and b) at 196 K; the descriptions c and uc refer to complexed and uncomplexed $CBPQT^{4+}$ components, respectively

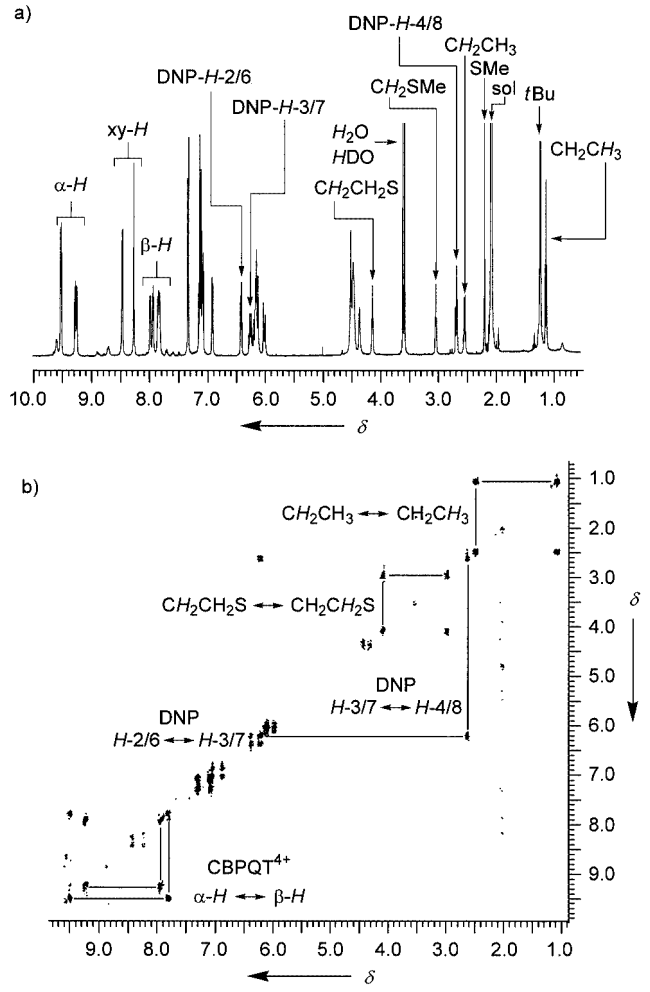

Figure 14. A sample of **5** (1 mM) in CD_3COCD_3 and 1.0 equivalent of $CBPQT^{4+}$ was prepared and the a) ^1H NMR spectrum (500 MHz) and b) ^1H DQF-COSY (500 MHz) recorded at 196 K

Table 5. Rate constants (k_{ex}) and derived free energies of activation ($\Delta G^{\ddagger}$) for the threading of $CBPQT^{4+}$ on the semidumbbell compound **5** determined by ^1H NMR spectroscopy in CD_3COCD_3 at different temperatures (T)

T [K][a]	k_{ex} [s^{-1}]	$t_{1/2}$ [s][b][c]	$\Delta G^{\ddagger}$ [kcal·mol^{-1}][a][d]
228	1	0.693	13.2
239	3	0.231	13.4
249	6	0.116	13.6
261	25	0.028	13.5
272	55	0.013	13.7
282	125	0.006	13.8

[a] Calibrated using neat MeOH sample, see: ref.[44]. [b] Experiments were performed with an initial concentration of the semidumbbell compound **5** of 1 mM containing 0.70 equiv. of $CBPQT^{4+}$. The k_{ex} values were obtained from partial line-shape analysis of the signal arising from the Me group in the ethyl substituent on the hydrophobic stopper using spin saturation transfer method, see: ref.[47] [c] The values for the "half-life" were obtained from $t_{1/2} = \ln 2/k_{ex}$. [d] Estimated error for $\Delta G^{\ddagger}$: ±0.1 kcal·mol^{-1}.

In order to determine an activation barrier for the complexation/decomplexation process occurring in **5**⊂$CBPQT^{4+}$, a CD_3COCD_3 solution of the semidumbbell compound **5** containing 0.70 equivalents of $CBPQT^{4+}$ was studied by VT ^1H NMR spectroscopy. Partial line-shape analysis[30] of the signals corresponding to the ^1H NMR signals for the ethyl group of the hydrophobic stopper as a function of temperature provided a series of rate constants (Table 5) for the complexation/decomplexation process.

Thermodynamic Parameters

Since, the $\Delta G^{\ddagger}$ values have been determined at different temperatures, the enthalpic ($\Delta H^{\ddagger}$) and entropic ($\Delta S^{\ddagger}$) contributions to the threading process leading to the formation of **3**⊂$CBPQT^{4+}$ and **5**⊂$CBPQT^{4+}$ can be calculated from plots (Figure 15) of $\Delta G^{\ddagger}$ against T. The kinetic parameters obtained from these plots and the values obtained[15,31] for the [2]rotaxanes $\mathbf{1}^{4+}$ and $\mathbf{2}^{4+}$ are summarized in Table 6,

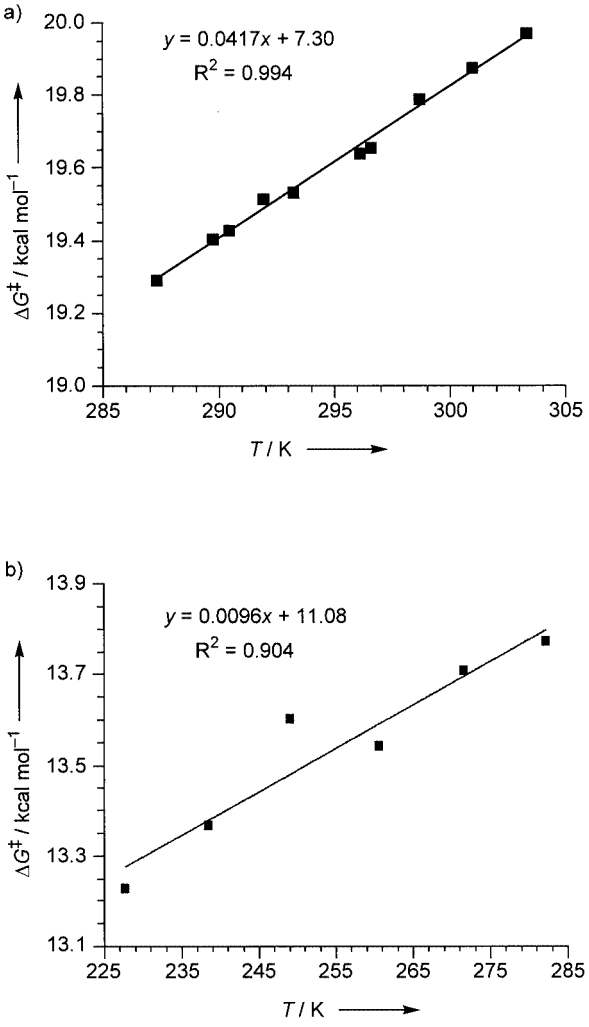

Figure 15. a) A linear plot of $\Delta G^{\ddagger}$ against T for the complexation of the semidumbbell compound **3** by $CBPQT^{4+}$; the $\Delta G^{\ddagger}$ values were obtained as described in Table 4; b) a linear plot of $\Delta G^{\ddagger}$ against T for the complexation of the semidumbbell compound **5** by $CBPQT^{4+}$; the $\Delta G^{\ddagger}$ values were obtained as described in Table 5

Table 6. Kinetic and thermodynamic parameters for shuttling of $CBPQT^{4+}$ in the [2]rotaxanes $\mathbf{1}^{4+}$ and $\mathbf{2}^{4+}$ and for the threading processes of $CBPQT^{4+}$ and the semidumbbell compounds **3**−**5**, leading to the formation of the [2]pseudorotaxanes **3**⊂$CBPQT^{4+}$, **4**⊂$CBPQT^{4+}$, and **5**⊂$CBPQT^{4+}$, respectively. Temperature 297 K, unless otherwise stated

Compound/Complex	k[a] [s^{-1}]	$t_{1/2}$[a] [s][b]	$\Delta G^{\ddagger}$[a] [kcal·mol^{-1}]	$\Delta H^{\ddagger}$[b] [kcal·mol^{-1}]	$\Delta S^{\ddagger}$[b] [cal·mol^{-1}·K^{-1}]
$\mathbf{1}^{4+}$	2.0×10^{-5}	35000	24.0	17	−24
$\mathbf{2}^{4+}$	60[c]	0.012[c]	14.8[c]	–	–
3⊂$CBPQT^{4+}$	2.0×10^{-2}	35	19.7	7.3	−42
4⊂$CBPQT^{4+}$	89[d]	0.008[d]	11.7[d]	–	–
5⊂$CBPQT^{4+}$	125[e]	0.006[e]	13.8[e]	11	−10

[a] The k, $t_{1/2}$, and $\Delta G^{\ddagger}$ values were obtained as described in Table 4 for **3**⊂$CBPQT^{4+}$ and as described in ref.[15] and ref.[31] for $\mathbf{1}^{4+}$. In the case of **4**⊂$CBPQT^{4+}$ and **5**⊂$CBPQT^{4+}$, the k, $t_{1/2}$, and $\Delta G^{\ddagger}$ values are given at the coalescence temperatures. [b] The $\Delta H^{\ddagger}$ and $\Delta S^{\ddagger}$ values were obtained from the intercept and slope of the straight line in the plot of $\Delta G^{\ddagger}$ against T, using the relationship $\Delta G^{\ddagger} = \Delta H^{\ddagger} - T\Delta S^{\ddagger}$, where T is the absolute temperature. [c] At 293 K. [d] At 238 K. [e] At 282 K.

together with the $\Delta G_c^{\ddagger}$ values reported for the threading process leading to the formation of **4**⊂$CBPQT^{4+}$.

Discussion of Kinetic and Thermodynamic Parameters

Knowledge of the thermodynamic parameters associated with the shuttling of the macrocyclic ring component $CBPQT^{4+}$ between the MPTTF and DNP recognition sites is of crucial importance in view of the use[8] of bistable [2]rotaxanes in the construction of devices. In the case of the slow bistable [2]rotaxane $\mathbf{1}^{4+}$, the rate-limiting step for the shuttling of $CBPQT^{4+}$ between the MPTTF and DNP recognition sites is the passage of $CBPQT^{4+}$ over the SMe group attached to the MPTTF unit. Replacement of this SMe group with a hydrogen atom, as in the bistable [2]rotaxane $\mathbf{2}^{4+}$, is therefore expected to lower the activation barrier considerably. Inspection of the data in Table 6 reveal that this is indeed the case, since the activation barrier for the process whereby the $CBPQT^{4+}$ ring component shuttles between the MPTTF and the DNP recognition sites is significantly lower (9.2 kcal·mol^{-1}) in the case of $\mathbf{2}^{4+}$. This observation is also reflected when comparing the processes whereby a $CBPQT^{4+}$ ring threads onto the MPTTF in the hydrophilic semidumbbell model compounds **3** and **4**.

A comparison (Table 6) of the kinetic and thermodynamic data obtained for the [2]rotaxane $\mathbf{1}^{4+}$ and the [2]pseudorotaxane **3**⊂$CBPQT^{4+}$ reveals that $\Delta H^{\ddagger}$ is much lower (9.7 kcal·mol^{-1}) in the case **3**⊂$CBPQT^{4+}$. This observation can be explained by the fact that $CBPQT^{4+}$, in the case of $\mathbf{1}^{4+}$, has to pass both an SMe group and a more bulky thioalkyl group before encircling the MPTTF unit, as compared with two SMe group in the case of **3**⊂$CBPQT^{4+}$. Although the $\Delta S^{\ddagger}$ value is negative in both $\mathbf{1}^{4+}$ and **3**⊂$CBPQT^{4+}$, the value is approximately twice as large in the case of **3**⊂$CBPQT^{4+}$, which can be explained by the fact that the threading process, leading to the formation of **3**⊂$CBPQT^{4+}$, involves the assembly of two separate components, whereas, in the shuttling process occurring in $\mathbf{1}^{4+}$, only one species is involved.

Binding Studies

To shed more light on the factors influencing the relative populations of the two translational isomers in the bistable [2]rotaxanes $\mathbf{1}^{4+}$ and $\mathbf{2}^{4+}$ and to get a better understanding of the thermochromic behavior observed in these compounds, detailed binding studies between the model semidumbbell compounds **3**−**5** and $CBPQT^{4+}$ have been carried out in Me_2CO. The outcome of investigations such as these is likely to be of fundamental importance in designing future bistable molecular switches.

3⊂*CBPQT*$^{4+}$

As a consequence of the high activation barrier leading to the formation (Scheme 3) of **3**⊂$CBPQT^{4+}$, the hydrophilic semidumbbell compound **3** was observed to be in slow exchange with its $CBPQT^{4+}$ complex on the ^{1}H NMR timescale (300 MHz) over a wide temperature range, allowing the binding constants between **3** and $CBPQT^{4+}$ to be determined at different temperatures by employing the ^{1}H NMR single-point method.[26,32] A CD_3COCD_3 solution (1.1 mM) containing equimolar amounts of **3** and $CBPQT^{4+}$ was subjected to VT ^{1}H NMR spectroscopic analysis (300 MHz). At each temperature, the solution was allowed to equilibrate for 1 h before the ^{1}H NMR spectrum was recorded. Several of the protons in the semidumbbell component show significant shifts in their resonances upon complexation. However, none of these signals were useful as probes for measuring K_a values, since they overlap other signals. The most diagnostic evidence which indicates that $CBPQT^{4+}$ encircles the MPTTF unit is the downfield shift[33] of the resonance for the SMe protons. At 298 K, this signal is observed as a singlet at δ = 2.64 ppm in **3**⊂$CBPQT^{4+}$, compared with a singlet resonating at δ = 2.45 ppm in the uncomplexed semidumbbell compound **3**. However, at higher temperatures, the singlet for the SMe protons in **3**⊂$CBPQT^{4+}$ begins to overlap the intense signal associated with the H_2O resonances therefore preventing exact integration of the SMe signal. The cyclophane protons also show significant shifts in their resonances upon complexation, and the signals associated with the $^+NCH_2$ and *p*-xylylene protons were found to be useful as probes.[34] The binding constants and derived free energies of complexation[35] ($-\Delta G^{\circ}$) obtained from these experiments are listed in Table 7.

Table 7. Binding constants (K_a values) and derived free energies of complexation[35] ($-\Delta G°$) between $CBPQT^{4+}$ and the semidumbbell compound **3** in CD_3COCD_3 determined using the ^1H NMR single-point method at different temperatures employing the $^+NCH_2$ and *p*-xylylene (xy-*H*) protons as probes

	$^+NCH_2$			*xy*-H				
T [K]	I_c	I_u	K_a [M^{-1}][a]	I_c	I_u	K_a [M^{-1}][a]	K_a (average) [M^{-1}]	$-\Delta G°$ [kcal·mol^{-1}]
298	1.00	3.05	400	1.00	2.74	450	425	3.58
302	1.00	3.39	350	1.00	2.95	410	380	3.56
306	1.00	3.75	310	1.00	3.13	380	345	3.55
310	1.00	4.01	280	1.00	3.47	340	310	3.53
314	1.00	4.34	260	1.00	3.78	300	280	3.51
318	1.00	4.64	240	1.00	4.15	270	255	3.50
322	1.00	5.13	210	1.00	4.60	240	225	3.46

[a] Estimated error on K_a: ±15%.

4⊂CBPQT^{4+}

Mixing equimolar amounts (0.75 mM) of the yellow semidumbbell compound **4** and the colorless $CBPQT^{4+}$ ring component in Me_2CO leads to the immediate formation (Scheme 4) of the [2]pseudorotaxane **4**⊂$CBPQT^{4+}$, as evidenced by the spontaneous production of a green-colored solution. The absorption spectrum (Figure 16) recorded at 297 K of this Me_2CO solution shows a broad band centered at 825 nm arising from the CT interactions that occur when $CBPQT^{4+}$ encircles[21] the MPTTF unit. An increase in the temperature of the green solution results (Figure 16) in a decrease in the intensity of the MPTTF/$CBPQT^{4+}$ CT band. The reverse is true on decreasing the temperature. UV/Vis dilution experiments were carried out at several different temperatures to determine the temperature dependence of the binding constants for the 1:1 complexation of $CBPQT^{4+}$ with the semidumbbell compound **4** in Me_2CO. The binding constants were obtained by correlating[21c] the maximum absorption of the MPTTF/$CBPQT^{4+}$ CT band with the absolute concentrations of the components.[26] The K_a and derived $-\Delta G°$ values,[35] obtained from these UV/Vis dilution experiments, are presented in Table 8, together with the molar extinction coefficients (ε).

Table 8. Binding constants (K_a values) and derived free energies of complexation[35] ($-\Delta G°$) between $CBPQT^{4+}$ and the semidumbbell compound **4**, determined by absorption spectroscopy in Me_2CO at different temperatures using the MPTTF/$CBPQT^{4+}$ CT band as probe

T [K]	$\lambda_{max.}$ [nm]	Data Points	Correlation Coefficient	ε [L·mol^{-1}·cm^{-1}]	K_a [M^{-1}][a]	$-\Delta G°$ [kcal·mol^{-1}]
287	825	12	0.999	1120	8300	5.14
292	825	11	0.999	1160	5700	5.01
297	825	11	0.998	1200	3950	4.89
302	825	10	0.999	1290	2500	4.69
307	825	9	0.999	1330	1800	4.57
312	825	8	1.000	1400	1250	4.42
317	825	8	0.998	1450	900	4.28

[a] Estimated error on K_a: ±15%.

5⊂CBPQT^{4+}

Mixing equimolar proportions (0.91 mM) of the colorless hydrophobic semidumbbell compound **5** and the colorless $CBPQT^{4+}$ ring component in Me_2CO at 299 K leads (Scheme 5) to the formation of the [2]pseudorotaxane **5**⊂$CBPQT^{4+}$, as indicated by the immediate appearance of a red-colored solution, which is related to the presence of a broad CT absorption band centered at 520 nm in the absorption spectrum (Figure 17). This band is characteristic[22] of superstructures containing a DNP moiety located inside $CBPQT^{4+}$. Just as in the case of the [2]pseudorotaxane **4**⊂$CBPQT^{4+}$, the absorption spectrum (Figure 17) re-

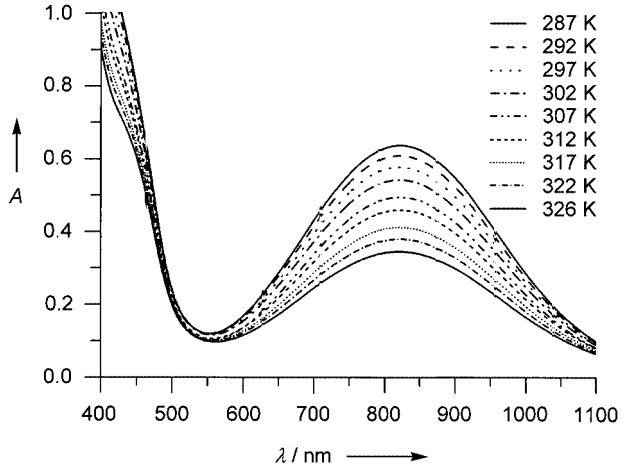

Figure 16. Absorption spectra recorded on a 1:1 mixture (0.75 mM) of the semidumbbell compound **4** and $CBPQT^{4+}$ in Me_2CO at different temperatures

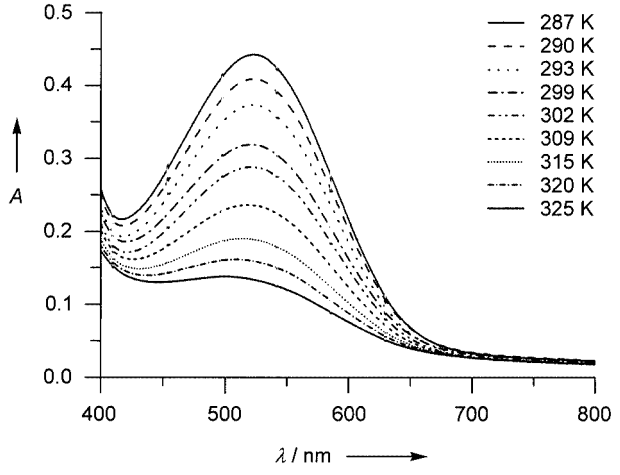

Figure 17. Absorption spectra recorded on a 1:1 mixture (0.91 mM) of the semidumbbell compound **5** and $CBPQT^{4+}$ in Me_2CO at different temperatures

corded on a 1:1 mixture of the semidumbbell compound **5** is strongly temperature dependent. The K_a and derived $-\Delta G°$ values[35] for the 1:1 complexation between $CBPQT^{4+}$ and compound **5** were obtained (Table 9) in Me_2CO at several different temperatures by UV/Vis dilution experiments, by using the DNP/$CBPQT^{4+}$ CT band as the probe.

Table 9. Binding constants (K_a values) and derived free energies of complexation[35] ($-\Delta G°$) between $CBPQT^{4+}$ and the semidumbbell compound **5**, determined by absorption spectroscopy in Me_2CO at different temperatures using the DNP/$CBPQT^{4+}$ CT band as probe

T [K]	$\lambda_{max.}$ [nm]	Data Points	Correlation Coefficient	ε [L·mol^{-1}·cm^{-1}]	K_a [M^{-1}][a]	$-\Delta G°$ [kcal·mol^{-1}]
287	520	9	0.989	790	2350	4.42
290	520	8	0.989	830	1600	4.25
293	520	6	0.999	840	1150	4.11
296	520	5	0.997	920	800	3.93
300	520	5	0.994	1010	570	3.77
302	520	5	0.987	1040	440	3.66
305	520	5	0.998	1070	350	3.55

[a] Estimated error on K_a: ±15%.

Thermodynamic Parameters

By constructing plots (Figure 18) of $\Delta G°$ against T for the complexation of the semidumbbell compounds **3**–**5** by $CBPQT^{4+}$, the enthalpic ($\Delta H°$) and entropic ($\Delta S°$) contributions to the formation of **3**⊂$CBPQT^{4+}$, **4**⊂$CBPQT^{4+}$, and **5**⊂$CBPQT^{4+}$ can be determined. Straight lines, each with a good fit, can be approximated to the experimental data, and the thermodynamic parameters obtained are summarized in Table 10.

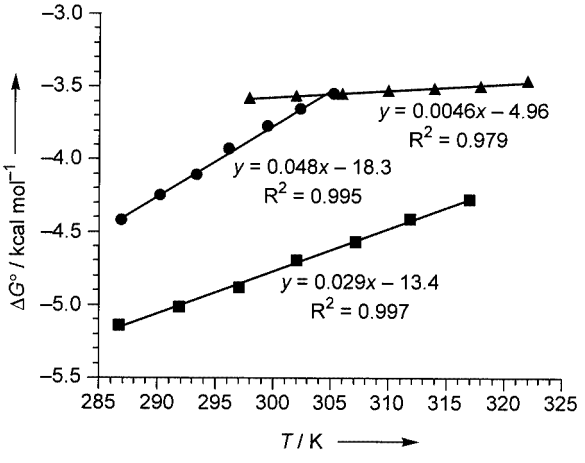

Figure 18. Linear plots of $\Delta G°$ against T for the complexation of the semidumbbell compounds **3** (solid triangles), **4** (solid squares), and **5** (solid circles) by $CBPQT^{4+}$ in Me_2CO (CD_3COCD_3)

Table 10. Binding constants (K_a values) and thermodynamic parameters for the complexation between $CBPQT^{4+}$ and the semidumbbell compounds **3**–**5** in Me_2CO at 302 K

Complex	K_a[a] [M^{-1}]	$-\Delta G°$[a] [kcal·mol^{-1}]	$-\Delta H°$[b] [kcal·mol^{-1}]	$-\Delta S°$[b] [cal·mol^{-1}·K^{-1}]
3⊂$CBPQT^{4+}$	380	3.56	5.0	4.6
4⊂$CBPQT^{4+}$	2500	4.69	13.4	29
5⊂$CBPQT^{4+}$	440	3.66	18.3	48

[a] The K_a and $\Delta G°$ values were obtained as described in Tables 7–9. [b] The $\Delta H°$ and $\Delta S°$ values were obtained from the intercept and slope of the straight line in the plot of $\Delta G°$ against T, using the relationship $\Delta G° = \Delta H° - T\Delta S°$, where T is the absolute temperature.

Discussion of Thermodynamic Parameters

A fundamental understanding of the noncovalent bonding interactions between $CBPQT^{4+}$ and the MPTTF and DNP recognition sites is of crucial importance in view of the possible applications of bistable [2]rotaxanes in the construction of devices and to aid the design of improved bistable [2]rotaxanes. In the bistable [2]rotaxane $\mathbf{1}^{4+}$, it was found[15] that the two translational isomers **1**·$GREEN^{4+}$ and **1**·RED^{4+} were present in a 1:1 ratio in Me_2CO at 300 K, an observation which suggests that the two major sets of noncovalent bonding interactions between $CBPQT^{4+}$ and the MPTTF and DNP recognition sites are of similar magnitudes. It is evident from Figure 18 and the data in Table 10 that the noncovalent bonding interactions between $CBPQT^{4+}$ and the hydrophilic semidumbbell compound **3** and the hydrophobic semidumbbell compound **5**, respectively, have the same strength at 302 K. These results are in perfect agreement with the fact that $\mathbf{1}^{4+}$ exist as a 1:1 mixture of **1**·$GREEN^{4+}$ and **1**·RED^{4+} in Me_2CO at this temperature. In the case of the bistable [2]rotaxane $\mathbf{2}^{4+}$, the ^{1}H NMR spectroscopic findings suggest that $\mathbf{2}^{4+}$ exists approximately as 50% **2**·$GREEN^{4+}$ and 50% **2**·RED^{4+} in Me_2CO at 273 K. The binding studies carried out on the model complexes **4**⊂$CBPQT^{4+}$ and **5**⊂$CBPQT^{4+}$ reveal that the free energy difference ($\Delta\Delta G°$) between the complexation ability of $CBPQT^{4+}$ with the separate MPTTF and DNP units of $\mathbf{2}^{4+}$ is about 0.3 kcal·mol^{-1}. Assuming that the relative distribution between **2**·$GREEN^{4+}$ and **2**·RED^{4+} is related to this free energy difference, one can calculate[36] that the equilibrium constant (K_{eq}) between **2**·$GREEN^{4+}$ and **2**·RED^{4+} is approximately 1.5. This K_{eq} value implies that the calculated amounts of **2**·$GREEN^{4+}$ and **2**·RED^{4+} is 60% and 40%, respectively, in Me_2CO at 273 K, which are in good agreement with the observed proportion of **2**·$GREEN^{4+}$ and **2**·RED^{4+} in the [2]rotaxane.

A comparison (Table 10) of the thermodynamic parameters for the model complexes **4**⊂$CBPQT^{4+}$ and **5**⊂$CBPQT^{4+}$ reveal that, while (1) the formation of **5**⊂$CBPQT^{4+}$ is more enthalpically favorable than the assembly of **4**⊂$CBPQT^{4+}$, (2) entropy factors favor the assembly of **4**⊂$CBPQT^{4+}$ more than the formation **5**⊂$CBPQT^{4+}$. Both complexes are stabilized by CT and

$\pi-\pi$ stacking interactions between their respective donor units and the electron-accepting bipyridinium units present in CBPQT^{4+} ring component. In the case of **5**⊂CBPQT^{4+}, the DNP-*H*-4/8 protons of the encircled DNP moiety also participate in [C−H···π] interactions with the π-faces of the *p*-xylylene units of CBPQT^{4+}, which probably further stabilize the **5**⊂CBPQT^{4+} complex enthalpically. However, this additional [C−H···π] enthalpic stabilization results in a significant loss of translational, rotational, and vibrational degrees of freedom in both CBPQT^{4+} and the DNP moiety, and therefore probably contributes negatively to the total entropy of formation for **5**⊂CBPQT^{4+}.

Electrochemical Investigations

These were carried out in nitrogen-purged MeCN solutions at room temperature by cyclic voltammetry (CV) and differential pulse voltammetry (DPV). Our studies have mainly focussed on the oxidation processes of the MPTTF units contained in the semidumbbell and dumbbell components.

Semidumbbells and Dumbbells

The hydrophilic semidumbbell compounds **3** and **4** contain one MPTTF electron-donating unit and a hydrophilic stopper. They both show (Figure 19, a and Figure 20, a) two reversible, monoelectronic oxidation processes, associated with the MPTTF unit and, at more positive potentials (>1.25 V vs. SCE), irreversible oxidation processes associated with the hydrophilic stopper. A comparison of the results obtained (Table 11) shows that the first oxidation process, associated with the MPTTF unit in the semidumbbell compound **4**, takes place at a potential that is less positive than that observed for the semidumbbell compound **3**. This cathodic shift (20 mV) is a consequence of replacing one of the electron-withdrawing SMe groups on the MPTTF unit with a hydrogen atom. The hydrophobic semidumbbell compound **5** contains one DNP electron-donating unit and a hydrophobic stopper. As expected, it shows (Figure 21, a and Table 11) one irreversible monoelectronic oxidation process associated with the DNP moiety and, at more positive potentials (> 1.35 V vs. SCE), irreversible oxidation processes associated with the hydrophobic stopper.

In common with semidumbbell compound **4**, the dumbbell compound **16** shows (Figure 22, a) two reversible, monoelectronic oxidation processes, associated with the MPTTF unit. However, the results obtained (Table 11) reveal that both the first and the second oxidation processes associated with the MPTTF unit in the dumbbell compound **16** take place at a potential that is less positive than those observed for compound **4**. This behavior can be attributed to the presence of stabilizing interactions between both the MPTTF$^{+\cdot}$ and MPTTF^{2+} and the DNP moiety[15b,37] present in **16**. Besides the MPTTF-based processes, compound **16** shows, at more positive potentials (> 1.25 V vs. SCE), irreversible processes that can be attributed to the oxidation of the DNP moiety, as well as to the phenoxy units present in the two stoppers. Unfortunately,

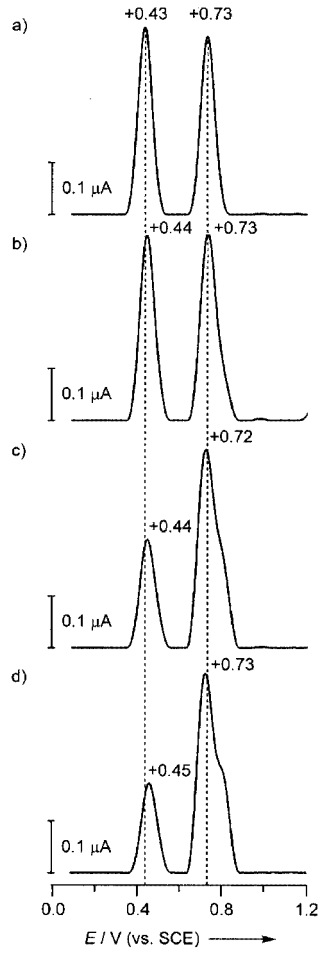

Figure 19. Differential pulse voltammograms (DPVs) recorded in MeCN at 298 K on a) the semidumbbell compound **3** (0.17 mM), b) **3** and 10 equiv. CBPQT^{4+} immediately after mixing, c) **3** and 10 equiv. CBPQT^{4+} 15 min after mixing, and d) **3** and 10 equiv. CBPQT^{4+} 24 h after mixing

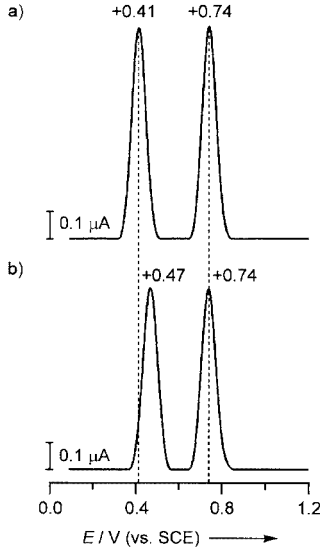

Figure 20. Differential pulse voltammograms (DPVs) recorded in MeCN at 298 K on a) the semidumbbell compound **4** (0.15 mM) and b) **4** and 10 equiv. CBPQT^{4+}

Table 11. Electrochemical data[a] for the semidumbbell compounds **3**−**5**, the dumbbell compound **16**, the [2]pseudorotaxanes **3**⊂CBPQT^{4+}, **4**⊂CBPQT^{4+}, and **5**⊂CBPQT^{4+}, and the [2]rotaxane **2**$^{4+}$

Compound/Complex	MPTTF[b] E_{ox} [V][c]		DNP[b] E_{ox} [V][d]
3	+0.43	+0.73	−
4	+0.41	+0.74	−
5	−	−	+1.18
16	+0.37	+0.72	−
2^{4+}	+0.50	+0.77[e]	−
3⊂CBPQT^{4+}	+0.73[e]	+0.79[e]	−
4⊂CBPQT^{4+}	+0.47	+0.74	−
5⊂CBPQT^{4+}	−	−	+1.20

[a] Nitrogen-purged MeCN, room temperature and tetrabutylammonium hexafluorophosphate ($TBAPF_6$) as supporting electrolyte, platinum disk as working electrode. Potential values in V vs. SCE. [b] Units involved in the observed processes. [c] Reversible and monoelectronic processes, unless otherwise indicated. [d] Irreversible process. [e] Overlapping of processes. For more details, see the text.

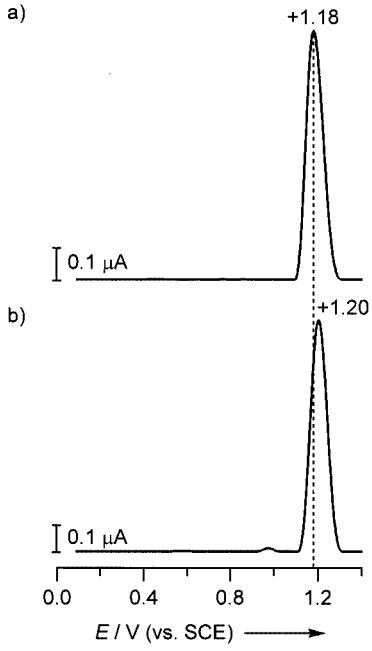

Figure 21. Differential pulse voltammograms (DPVs) recorded in MeCN at 298 K on a) the semidumbbell compound **5** (0.10 mM) and b) **5** and 10 equiv. CBPQT^{4+}

the first irreversible oxidation of the hydrophilic dendritic stopper take place at a potential similar to that of the DNP moiety, preventing us from obtaining any useful information about the precise location of the oxidation potential of the DNP moiety incorporated in the dumbbell compound **16**. However, in the semidumbbell compound **14**, the precursor to the semidumbbell compound **16**, the hydrophilic stopper is absent, and the irreversible oxidation process of the DNP moiety can be observed. This occurs at +1.30 V (vs. SCE) and is anodically shifted (120 mV) relative to that of the semidumbbell compound **5**. This behavior can be attributed to the fact that oxidation of the DNP moiety in the semidumbbell compound **14** can only occur after dioxidation of the MPTTF unit. As a consequence of Coulombic repulsion between the MPTTF^{2+} and the DNP$^{+\cdot}$ moiety, oxidation of the DNP moiety is rendered more difficult when it is incorporated into the semidumbbell compound **14**.

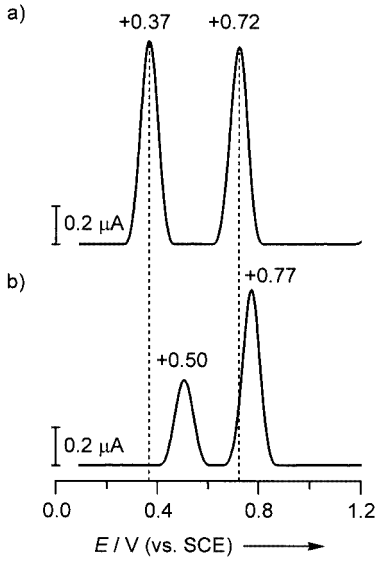

Figure 22. Differential pulse voltammograms (DPVs) recorded in MeCN at 298 K on a) the dumbbell compound **16** (0.5 mM) and b) the [2]rotaxane **2**$^{4+}$ (0.5 mM)

[2]Pseudorotaxane 3⊂CBPQT^{4+}

The process whereby CBPQT^{4+} threads onto the MPTTF unit contained in the semidumbbell compound **3** could also be followed (Figure 19) by monitoring the changes in the position and the shape of the DPV peaks. Figure 19 (b) shows the DPV recorded on a MeCN solution containing 0.15 mM of **3** and excess (10 equivalents) CBPQT^{4+} immediately after its preparation. A comparison of the DPV peaks in Figure 19 (a and b) shows almost no changes in the position and shape of the DPV peaks, indicating that the MeCN solution contains at this stage almost exclusively uncomplexed species, namely, the semidumbbell compound **3** and CBPQT^{4+}. As time progresses (Figure 19, c and d), and CBPQT^{4+} starts to thread onto the MPTTF unit, a significant decrease in the current intensities of the first DPV peak, centered around +0.44 V (vs. SCE) is observed. Moreover, this decrease in the current intensities is accompanied by the formation of a shoulder on the right side of the second DPV peak, centered around +0.73 V (vs. SCE). After 24 h at room temperature, the system had equilibrated and no perceptible changes were observed in the voltammograms recorded subsequently. These observations can be explained by the slow formation of **3**⊂CBPQT^{4+}. The peak observed at +0.45 V in Figure 19 (d) can be attributed to the first oxidation process of the MPTTF unit in the uncomplexed semidumbbell compound **3**, whereas the peak observed around +0.73 V is a result of

overlapping processes and can be assigned to the second oxidation (+0.73 V) of the MPTTF unit in the uncomplexed semidumbbell compound **3** and to the first (+0.73 V) and second (+0.79 V) oxidations of the MPTTF unit in **3**⊂CBPQT^{4+}. The large shift of 300 mV toward more positive potentials for the first oxidation process of the MPTTF unit in **3**⊂CBPQT^{4+} shows that the MPTTF unit is engaged in strong CT interactions with the two-electron-accepting bipyridinium units in CBPQT^{4+}. In the case of **4**⊂CBPQT^{4+}, a much smaller anodic shift (60 mV) is observed (vide infra) when comparing the first oxidation process associated with the MPTTF unit in **4** and **4**⊂CBPQT^{4+}. These results indicate that the [2]pseudorotaxane **3**⊂CBPQT^{4+} has some [2]rotaxane character.[38]

[2]Pseudorotaxane 4⊂CBPQT^{4+}

The electrochemical investigations of **4**⊂CBPQT^{4+} were carried out in a MeCN solution containing the semidumbbell component and an excess of CBPQT^{4+} in order to avoid the presence of substantial amounts of free species.[39] The electrochemical data (Figure 20, b) for **4**⊂CBPQT^{4+} were obtained in a MeCN solution, containing the semidumbbell compound **4** (0.2 mM) and 10 equivalents of CBPQT^{4+}. A comparison (Figure 20 and Table 11) of the results obtained for **4** and **4**⊂CBPQT^{4+} show that, in the [2]pseudorotaxane **4**⊂CBPQT^{4+}, the first oxidation of the MPTTF unit is shifted (60 mV) toward more positive potentials with respect to that of compound **4**, whereas the second oxidation potential is unaffected by the presence of CBPQT^{4+}. These results can be explained[40] as follows: (1) In **4**⊂CBPQT^{4+}, the MPTTF unit is engaged in CT interactions with CBPQT^{4+} while, after the first oxidation of the MPTTF unit, (2) dethreading takes place because the noncovalent bonding interactions between the MPTTF$^{+\cdot}$ unit and CBPQT^{4+} are eradicated and a Coulombic repulsion is introduced between the mono-oxidized MPTTF$^{+\cdot}$ unit and CBPQT^{4+}. Consequently, (3) the second oxidation of the MPTTF$^{+\cdot}$ unit in the mixture of uncomplexed **4**$^{+\cdot}$ and uncomplexed CBPQT^{4+} takes place at the same potential as that of the second oxidation of the semidumbbell component.

[2]Pseudorotaxane 5⊂CBPQT^{4+}

Once again, the electrochemical investigations of **5**⊂CBPQT^{4+} were carried out in a MeCN solution containing the semidumbbell compound **5** (0.2 mM) and 10 equivalents of CBPQT^{4+} in order to avoid the presence of substantial amounts of free species. The electrochemical data (Figure 21 and Table 11), obtained for compound **5** and the [2]pseudorotaxane **5**⊂CBPQT^{4+}, reveal that the irreversible oxidation process associated with the DNP moiety in **5**⊂CBPQT^{4+} is slightly anodically shifted (20 mV) relative to the same process in compound **5**. This shift toward more positive potentials can be accounted for by the presence, in **5**⊂CBPQT^{4+}, of CT interactions between the DNP moiety and CBPQT^{4+}. As in the case of **4**⊂CBPQT^{4+}, dethreading takes place, in **5**⊂CBPQT^{4+}, after oxidation of the DNP moiety because the noncovalent interactions between the DNP moiety and CBPQT^{4+} are eradicated and a Coulombic repulsion is introduced between the oxidized DNP$^{+\cdot}$ unit and CBPQT^{4+}.

[2]Rotaxane 2^{4+}

The [2]rotaxanes **2**$^{4+}$ exists (vide supra) in MeCN solution as a mixture of two translational isomers (Scheme 2). In the potential range of MPTTF oxidation, **2**$^{4+}$ show (Figure 22 and Table 11) two processes that take place at +0.50 and +0.77 V vs. SCE. These two processes exhibit different CV current intensities and DPV peak areas. We can attribute the first peak at +0.50 V to the first oxidation of the MPTTF unit in **2**·RED^{4+} interacting[41] "alongside" with CBPQT^{4+}. The peak observed at +0.77 V arises from the overlapping of the first oxidation of the MPTTF unit in **2**·GREEN^{4+}, and to the second oxidation of the MPTTF unit in **2**$^{4+}$. As far as the translational isomer **2**·GREEN^{4+} is concerned, it is impossible to demonstrate unequivocally the occurrence of the expected ring shuttling after oxidation of the MPTTF unit, since both oxidation processes for the free and encircled DNP moieties overlap with the irreversible oxidation processes of the phenoxy units present in both the hydrophobic and hydrophilic stoppers. However, the electrochemical results obtained for the model [2]pseudorotaxane **4**⊂CBPQT^{4+} show that CBPQT^{4+} leaves the MPTTF station after the first oxidation. Together with this, the fact that in the [2]rotaxane **2**$^{4+}$ the second oxidation of the MPTTF unit is only slightly anodically shifted (50 mV), relative (Table 11) to the same process in its corresponding dumbbell component, seems to indicate that the [2]rotaxane **2**$^{4+}$, after the first oxidation of the MPTTF unit, consists of only one species, i.e. **2**·RED$^{5+\cdot}$. As a direct consequence hereof, shuttling of the tetracationic CBPQT^{4+} ring component must take place after the first oxidation of the MPTTF unit in **2**·GREEN^{4+}. The observed shift toward more positive potentials for the second oxidation of the MPTTF unit in the [2]rotaxane **2**$^{4+}$, compared with the same process for the dumbbell compound **16**, can be accounted for by (1) the presence of CBPQT^{4+}, which destroys the interactions of the oxidized MPTTF unit with the other electron-donating units present in the case of the dumbbell compound **16**, and (2) a Coulombic repulsion, which arises between the oxidized MPTTF unit and CBPQT^{4+}.

Chemical Switching Experiments

In order to investigate the ability to switch the [2]rotaxane **2**$^{4+}$ chemically, two model compounds were investigated to observe the changes in their ^{1}H NMR spectra upon oxidation. Compounds **20** and **21** were studied in CD_3CN solutions and their ^{1}H NMR spectra recorded (Figure 23, a and c, respectively). Addition of two equivalents of the oxidant, tris(*p*-bromophenyl)amminium hexafluoroantimonate, which was used in a previous study[9a] to oxidize substituted TTFs, to these solutions resulted in significant downfield shifts (Figure 23, b and d) of all of

the signals. The signals for the pyrrolo protons shift from δ = 6.6 and 6.6 ppm for **20** and **21** to δ = 7.5 and 7.6 ppm for $\mathbf{20}^{2+}$ and $\mathbf{21}^{2+}$, respectively. Addition of a reductant (zinc powder) restored the original spectra (not shown in Figure 23).

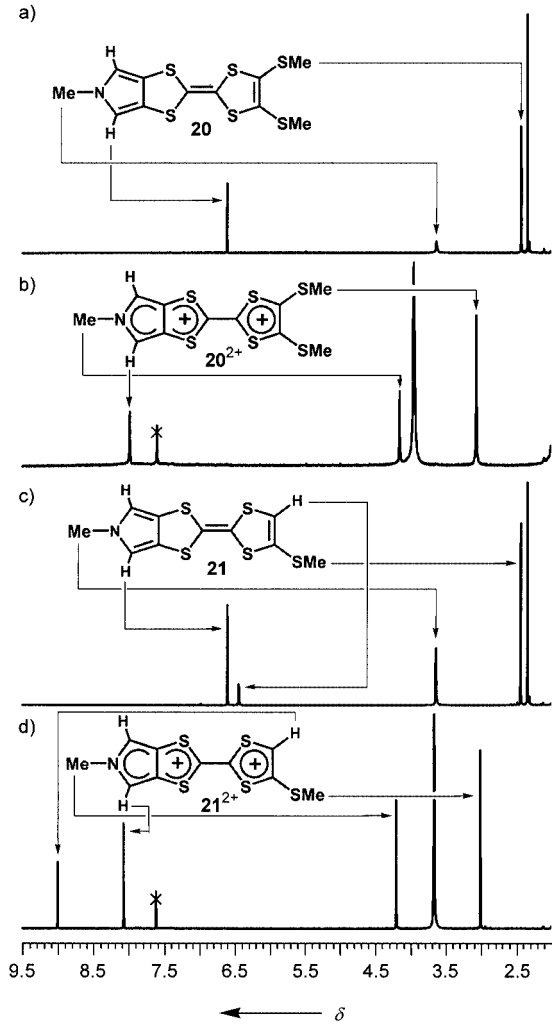

Figure 23. ^{1}H NMR spectra (500 MHz) in CD_3COCD_3 at 253 K of **20** a) before and b) after addition of two equivalents of the oxidant, tris(*p*-bromophenyl)amminium hexafluorantimonate, and **21** c) before and d) after addition of two equivalents of the oxidant

A similar experiment was performed on the [2]rotaxane $\mathbf{2}^{4+}$. The ^{1}H NMR spectrum (Figure 24, a) of a solution of $\mathbf{2}^{4+}$ in CD_3COCD_3 was recorded at 253 K. In this spectrum, the presence of both the RED and GREEN translational isomers can be seen clearly by the duplication of the signals, particularly those of the *tert*-butyl and Me protons on the hydrophobic stopper shown in the inset. Upon addition of two equivalents of the oxidant and recording the ^{1}H NMR spectrum again (Figure 24, b), a major change is observed. The spectrum is greatly simplified relative to the initial spectrum, reflecting the presence of only a single translational isomer − apparent on observation of the same signals for the hydrophobic stopper shown in the inset. This translational isomer can be assigned as the RED isomer on account of the signals at δ = 6.2, 5.9 and 2.3 ppm and so corresponding to the protons of a DNP unit encircled by $CBPQT^{4+}$.

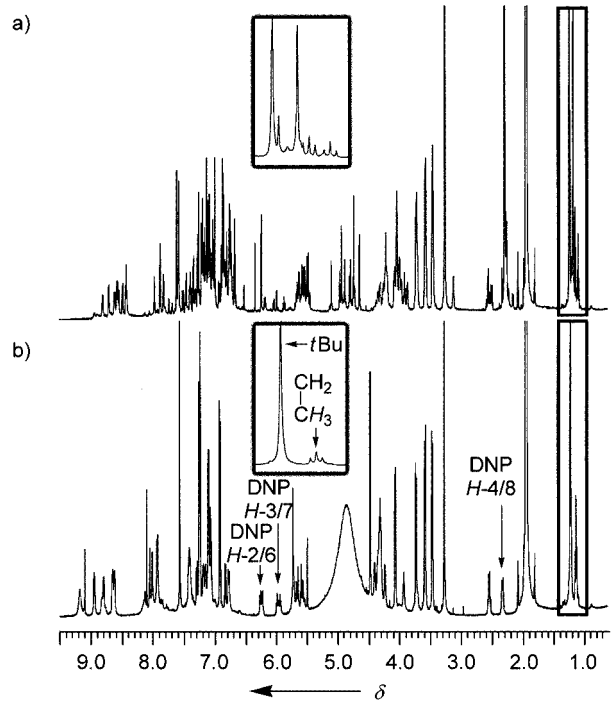

Figure 24. ^{1}H NMR spectra (500 MHz) in CD_3COCD_3 at 253 K of $\mathbf{2}^{4+}$ a) before and b) after addition of two equivalents of the oxidant, tris(*p*-bromophenyl)amminium hexafluorantimonate; the insets show the region from δ = 1.0 to 1.5 ppm expanded

Conclusion

Replacement of a thiomethyl speed bump in an amphiphilic bistable [2]rotaxane containing a (monopyrrolo)tetrathiafulvalene unit and a 1,5-dioxynaphthalene moiety with a hydrogen atom creates an open street for the passage of the tetracationic cyclobis(paraquat-*p*-phenylene) cyclophane. This simple constitutional modification not only reduces the barrier height to translational isomerization by about 10 kcal·mol^{-1}, but also creates a bias in favor of the green isomer, i.e. the tetracationic cyclophane resides for 80% of the time around the (monopyrrolo)tetrathiafulvalene unit in acetone at room temperature. The ground state of this bistable rotaxane allows switching of the major translational isomer to be carried out electrochemically as well as chemically. It is evident, therefore, that a very small change in the constitution of a switchable rotaxane can have a profound effect on its performance as a switch. The findings reported herein are undoubtedly not unimportant when it comes to the future design and construction of bistable [2]rotaxanes.[42]

Experimental Section

General Methods: Chemicals were purchased from Aldrich and were used as received, unless indicated otherwise. The compounds 5-tosyl-5*H*-1,3-dithiolo[4,5-*c*]pyrrol-2-one[18b] (**8**) (Scheme 1), 4-(2-cyanoethylthio)-1,3-dithiole-2-thione[19] (**9**) (Scheme 1), the semidumbbell compound[15b] **11**, (Scheme 1), compound[8b] **15** (Scheme 1), and 1,1′′-[1,4-phenylenebis(methylene)]bis(4,4′-bipyridin-1-ium) bis(hexafluorophosphate)[10a] (**17**·2PF_6) (Scheme 2), 2-[4,5-bis(methylthio)-1,3-dithiol-2-ylidene]-5*H*-1,3-dithiolo[4,5-*c*]pyrrole[18b] (**6**) (Scheme 3), and cyclobis(paraquat-*p*-phenylene) tetrakis(hexafluorophosphate)[24] (CBPQT·4PF_6) (Scheme 3−5) were all prepared according to literature procedures. Solvents were dried according to literature procedures.[43] All reactions were carried out under anhydrous nitrogen. High pressure experiments were carried out in a Teflon-tube with a Psika high pressure apparatus. Thin-layer chromatography (TLC) was carried out using aluminium sheets pre-coated with silica gel 60F (Merck 5554). The plates were inspected under UV light and, if required, developed in I_2 vapor. Column chromatography was carried out using silica gel 60F (Merck 9385, 0.040−0.063 mm). Melting points were determined on a Büchi melting point apparatus and are uncorrected. ^{1}H NMR spectra were recorded (at room temperature except where stated otherwise) with a Bruker Avance500 spectrometer (500 MHz) or on a Gemini-300BB instrument (300 MHz), using residual solvent as the internal standard. ^{13}C NMR spectra were recorded at room temperature with a Gemini-300BB instrument (75 MHz), using residual solvent as the internal standard. All chemical shifts are quoted on a δ scale, and all coupling constants (J) are expressed in Hertz (Hz). Samples were prepared using $CDCl_3$, CD_3COCD_3, CD_3CN or CD_3SOCD_3 purchased from Cambridge Isotope Labs. Temperatures were calibrated using a neat MeOH sample[44] before or after each experiment and assumed to remain constant during the experiment. Electron impact ionization mass spectrometry (EI-MS) was performed on a Varian MAT 311A instrument and matrix-assisted laser-desorption/ionization time-of-flight mass spectrometry (MALDI−TOF−MS) was performed on a Kratos Kompact MALDI−TOF instrument, utilizing a 2,5-dihydroxybenzoic acid matrix. Infrared (IR) spectra were recorded on a Perkin−Elmer 580 spectrophotometer. Microanalyses were performed by the Atlantic Microlab, Inc., Atlanta, Georgia.

2-[4-(2-Cyanoethylthio)-1,3-dithiol-2-ylidene]-5-tosyl-5*H*-1,3-dithiolo[4,5-*c*]pyrrole (10): The ketone **8** (1.48 g, 4.75 mmol) and the thione **9** (1.04 g, 4.74 mmol) were suspended in distilled $(EtO)_3P$ (35 mL) and heated to 135 °C (during heating the two solids dissolved leaving a red solution, and after 20−30 min a yellow orange precipitate was formed). Two additional portions of the thione **9** (á 0.52 g, 2.37 mmol) were added after 15 and 30 min. The red reaction mixture was stirred for 2 h at 135 °C and cooled to room temperature, and addition of MeOH (150 mL) yielded a yellow solid, which was filtered, washed with MeOH (3 × 150 mL) and dried in vacuo. The yellow solid was suspended in CH_2Cl_2 (40 mL) and subjected to column chromatography (SiO_2: CH_2Cl_2). (Before the column was eluted an almost insoluble yellow solid exclusively containing the symmetric bis(pyrrolo)TTF was removed carefully from the top of the column with a spatula). The yellow band (R_f = 0.4) was collected and the solvent evaporated to give a yellow solid, which was dissolved in CH_2Cl_2/MeOH (1:1 v/v, 400 mL) and concentrated to approximately half of its volume to precipitate the product. The yellow crystals were collected by filtration and dried in vacuo to give the title compound **10** (1.47 g, 64%) as a yellowish orange solid. M.p. 159−159.5 °C. ^{1}H NMR (CD_3SOCD_3, 300 MHz, ppm): δ = 2.38 (s, 3 H), 2.83 (t, J = 6.7 Hz, 2 H), 3.06 (t, J = 6.7 Hz, 2 H), 7.02 (s, 1 H), 7.38 (s, 2 H), 7.46 (d, J = 8.2 Hz, 2 H), 7.83 (d, J = 8.2 Hz, 2 H). ^{13}C NMR (CD_3SOCD_3, 75 MHz, ppm): δ = 17.8, 21.1, 30.4, 112.6 (2 signals), 114.6, 117.0, 118.8, 122.8, 125.6, 126.2, 126.3, 126.8, 130.4, 134.5, 145.8. MS (EI): m/z (%) = 482 (48) $[M]^+$, 327 (88) $[M - Ts]^+$, 273 (20), 184 (45), 91 (100). IR (KBr): $\tilde{\nu}$ = 2250 cm^{-1} (C≡N). $C_{18}H_{14}N_2O_2S_6$ (482.7): calcd. C 44.79, H 2.92, N 5.80, S 39.86; found C 44.58, H 2.94, N 5.72, S 39.75.

Compound 12: The bromide **11** (1.23 g, 1.43 mmol) was dissolved in anhydrous Me_2CO (80 mL) and NaI (3.22 g, 21.5 mmol) was added in one portion. The reaction mixture was heated under reflux for 3 days, before being cooled to room temperature and the solvent removed in vacuo. The white residue was dissolved in CH_2Cl_2 (100 mL) and washed with H_2O (3 × 100 mL) before being dried ($MgSO_4$). Concentration in vacuo gave the title compound **12** (1.28 g, 99%) as a white foam. ^{1}H NMR ($CDCl_3$, 300 MHz, ppm): δ = 1.22 (t, J = 7.6 Hz, 3 H), 1.29 (s, 18 H), 2.62 (q, J = 7.6 Hz, 2 H), 3.30 (t, J = 6.9 Hz, 2 H), 3.90 (t, J = 6.9 Hz, 2 H), 3.96−4.01 (m, 4 H), 4.03−4.07 (m, 2 H), 4.12−4.16 (m, 2 H), 4.26−4.33 (m, 4 H), 6.77−6.86 (m, 4 H), 7.03−7.10 (m, 10 H), 7.20−7.37 (m, 6 H), 7.86 (d, J = 8.5 Hz, 1 H), 7.87 (d, J = 8.5 Hz, 1 H). ^{13}C NMR ($CDCl_3$, 75 MHz, ppm): δ = 2.9, 15.3, 28.2, 31.4, 34.3, 63.1, 67.3, 67.9, 68.0, 69.4, 70.0, 70.1, 72.2, 105.7, 105.8, 113.1, 114.6, 114.8, 124.0, 125.1, 125.2, 126.6, 126.7, 126.8, 130.7, 131.0, 132.2, 139.8, 141.3, 144.1, 144.6, 148.3, 154.2, 154.3, 156.5. MS (MALDI−TOF): m/z (%) = 905 (100) $[M]^+$. $C_{53}H_{61}IO_5$ (905.0): calcd. C 70.34, H 6.79; found C 70.49, H 6.85.

Compound 13: A solution of compound **10** (0.36 g, 0.75 mmol) in anhydrous THF (50 mL) was degassed (N_2, 10 min) before a solution of CsOH·H_2O (0.13 g, 0.79 mmol) in anhydrous MeOH (6 mL) was added dropwise with a syringe over a period of 45 min at room temperature. The mixture was stirred for 15 min, whereupon a solution of the iodide **12** (0.72 g, 0.80 mmol) in anhydrous THF (10 mL) was added in one portion, and the reaction mixture was stirred for 24 h at room temperature. The solvent was evaporated and the resulting yellow brown residue was dissolved in CH_2Cl_2 (150 mL), washed with brine (100 mL), H_2O (2 × 100 mL) and dried ($MgSO_4$). Removal of the solvent gave a yellowish brown semisolid, which was purified by column chromatography (SiO_2: CH_2Cl_2/cyclohexane, 9:1). The broad yellow band (R_f = 0.3) was collected and concentrated, affording a yellow foam, which was repeatedly dissolved in CH_2Cl_2 (2 × 20 mL) and concentrated to give the title compound **13** (0.63 g, 70%) as a yellow foam. ^{1}H NMR (CD_3COCD_3, 300 MHz, ppm): δ = 1.20 (t, J = 7.6 Hz, 3 H), 1.29 (s, 18 H), 2.39 (s, 3 H), 2.61 (q, J = 7.6 Hz, 2 H), 3.03 (t, J = 6.4 Hz, 2 H), 3.83 (t, J = 6.4 Hz, 2 H), 3.94−3.98 (m, 4 H), 4.02−4.06 (m, 2 H), 4.15−4.19 (m, 2 H), 4.27−4.34 (m, 4 H), 6.68 (s, 1 H), 6.85 (d, J = 8.8 Hz, 2 H), 6.90−6.97 (m, 2 H), 7.06−7.14 (m, 10 H), 7.24 and 7.26 (AB q, J = 2.1 Hz, 2 H), 7.28−7.44 (m, 8 H), 7.82−7.86 (m, 4 H). MS (MALDI−TOF): m/z (%) = 1205 (22) $[M]^+$, 1051 (100) $[M + H - Ts]^+$. $C_{68}H_{71}NO_7S_6$ (1206.7): calcd. C 67.68, H 5.96, N 1.16, S 15.94; found C 67.45, H 5.99, N 1.27, S 15.65.

Compound 14: Compound **13** (0.53 g, 0.44 mmol) was dissolved in anhydrous THF/MeOH (1:1 v/v, 65 mL) and degassed (N_2, 10 min) before NaOMe (30% in MeOH, 1.25 mL, 0.35 g, 6.6 mmol) was added in one portion. The yellow solution was heated under reflux for 15 min before being cooled to room temperature, whereupon the solvent was evaporated. The yellow residue was dissolved in CH_2Cl_2 (100 mL), washed with H_2O (3 × 100 mL) and dried ($MgSO_4$). Concentration gave a yellowish orange foam, which was

subjected to column chromatography (SiO_2: CH_2Cl_2). The yellow band ($R_f = 0.4$) was collected and concentrated to provide the title compound **14** (0.39 g, 85%) as a yellow foam. ^1H NMR (CD_3COCD_3, 300 MHz, ppm): $\delta = 1.20$ (t, $J = 7.7$ Hz, 3 H), 1.30 (s, 18 H), 2.61 (q, $J = 7.7$ Hz, 2 H), 3.05 (t, $J = 6.4$ Hz, 2 H), 3.85 (t, $J = 6.4$ Hz, 2 H), 3.96−4.00 (m, 4 H), 4.02−4.05 (m, 2 H), 4.15−4.19 (m, 2 H), 4.29−4.34 (m, 4 H), 6.68 (s, 1 H), 6.78 (s, 2 H), 6.85 (d, $J = 9.3$ Hz, 2 H), 6.94 (d, $J = 7.8$ Hz, 1 H), 6.96 (d, $J = 7.7$ Hz, 1 H), 7.05−7.14 (m, 10 H), 7.27−7.39 (m, 6 H), 7.84 (d, $J = 8.6$ Hz, 1 H), 7.85 (d, $J = 8.8$ Hz, 1 H), 10.32 (br. s, 1 H). MS (MALDI−TOF): *m/z* (%) = 1051 (100) $[M]^+$. $C_{61}H_{65}NO_5S_5$ (1052.5): calcd. C 69.61, H 6.22, N 1.33, S 15.23; found C 69.47, H 6.15, N 1.42, S 15.07.

Dumbbell 16: Compound **14** (0.21 g, 0.20 mmol) and the chloride **15** (0.20 g, 0.22 mmol) were dissolved in anhydrous DMF (10 mL) and degassed (N_2, 10 min) before NaH (0.021 g of a 60% suspension in mineral oil, 0.53 mmol) was added. The reaction mixture was stirred for 50 min at room temperature, causing the initially yellow solution to become more orange. H_2O (40 mL) was added (dropwise until no more gas evolution was observed), followed by addition of brine (40 mL). The yellow precipitate was filtered, washed with H_2O (2 × 20 mL) and dried. The crude product was purified by column chromatography (SiO_2: CH_2Cl_2/EtOAc, 2:1). The yellow band ($R_f = 0.3$) was collected and the solvent evaporated affording a yellow oil, which was repeatedly dissolved in CH_2Cl_2 (2 × 20 mL) and concentrated to give the title compound **16** (0.27 g, 70%) as a yellow foam. ^1H NMR (CD_3COCD_3, 300 MHz, ppm): $\delta = 1.19$ (t, $J = 7.6$ Hz, 3 H), 1.29 (s, 18 H), 2.60 (q, $J = 7.6$ Hz, 2 H), 3.02 (t, $J = 6.4$ Hz, 2 H), 3.28 (s, 6 H), 3.29 (s, 3 H), 3.47−3.51 (m, 6 H), 3.62−3.66 (m, 6 H), 3.77−3.82 (m, 6 H), 3.83 (t, $J = 6.4$ Hz, 2 H), 3.92−4.02 (m, 6 H), 4.07−4.16 (m, 8 H), 4.26−4.30 (m, 4 H), 4.91 (s, 2 H), 4.98 (s, 2 H), 5.02 (s, 2 H), 5.03 (s, 4 H), 6.65 (s, 1 H), 6.73 and 6.75 (AB q, $J = 2.0$ Hz, 2 H), 6.81 (d, $J = 8.6$ Hz, 2 H), 6.83 (d, $J = 8.6$ Hz, 2 H), 6.85 (s, 2 H), 6.90−6.97 (m, 8 H), 7.05−7.14 (m, 10 H), 7.17 (d, $J = 8.7$ Hz, 2 H), 7.24−7.35 (m, 8 H), 7.38 (d, $J = 8.5$ Hz, 4 H), 7.83 (d, $J = 8.5$ Hz, 1 H), 7.84 (d, $J = 8.5$ Hz, 1 H). MS (MALDI−TOF): *m/z* (%) = 1920 (100) $[M]^+$, 1711 (15). $C_{111}H_{125}NO_{18}S_5$ (1921.5): calcd. C 69.38, H 6.56, N 0.73, S 8.34; found C 69.17, H 6.48, N 0.80, S 8.33.

"Fast" Bistable [2]Rotaxane (2·4PF$_6$): A solution of the dumbbell compound **16** (0.21 g, 0.11 mmol), **17**·2PF$_6$ (0.24 g, 0.34 mmol) and **18** (0.090 g, 0.34 mmol) in anhydrous DMF (12 mL) was transferred to a Teflon-tube and subjected to 10 kbar of pressure at room temperature for 3 days. The dark green solution was subjected directly to column chromatography (SiO_2) and unchanged **16** was eluted with Me_2CO, whereupon the eluent was changed to Me_2CO/NH_4PF_6 (1.0 g NH_4PF_6 in 100 mL Me_2CO) and the dark green band was collected. Most of the solvent was removed in vacuo ($T < 30$ °C) followed by addition of H_2O (100 mL). The resulting precipitate was collected by filtration, washed with H_2O (2 × 20 mL) and Et_2O (2 × 25 mL) before being dried (P_2O_5), affording the title [2]rotaxane **2**·4PF$_6$ (0.18 g, 55%) as a dark green solid. M.p. 155 °C (decomposed without melting). The data given below are for the mixture of the two translational isomers. MS (MALDI−TOF): *m/z* (%) = 2585 (4) $[M - 3PF_6]^+$, 2440 (2) $[M - 4PF_6]^+$, 1920 (1), 665 $[CBPQT{\cdot}PF_6]^+$ (18), 561 (100). UV/Vis (Me_2CO, 298 K): $\lambda_{max.}$ (ε) = 520 (850), 815 nm (1410 L·mol^{-1}·cm^{-1}). UV/Vis (MeCN, 298 K): $\lambda_{max.}$ (ε) = 520 (850), 825 nm (1820 L·mol^{-1}·cm^{-1}). UV/Vis (Me_2SO, 298 K): $\lambda_{max.}$ (ε) = 520 (640), 788 nm (1090 L·mol^{-1}·cm^{-1}). $C_{147}H_{157}F_{24}N_5O_{18}P_4S_5{\cdot}2H_2O$ (3022.0): calcd. C 57.74, H 5.31, N 2.29, S 5.24; found C 57.70, H 5.37, N 2.49, S 5.08.

All attempts to separate the two translational isomers by employing PTLC failed on account of the fast shuttling of $CBPQT^{4+}$ between the two recognition sites in **2**·4PF$_6$. However, **2**·4PF$_6$·RED was characterized as a consequence of the fact in CD_3COCD_3 solution at 215 K, **2**·4PF$_6$ exists almost exclusively as **2**·4PF$_6$·RED.

Data for 2·4PF$_6$·RED: ^1H NMR (CD_3COCD_3, 500 MHz, 215 K, ppm): $\delta = 1.08$ (t, $J = 7.6$ Hz, 3 H), 1.17 (s, 18 H), 2.49 (q, $J = 7.6$ Hz, 2 H), 2.53 (d, $J = 8.0$ Hz, 1 H), 2.54 (d, $J = 8.0$ Hz, 1 H), 3.19 (s, 3 H), 3.23 (s, 6 H), 3.40−3.47 (m, 10 H), 3.55−3.61 (m, 6 H), 3.72−3.77 (m, 6 H), 3.97−4.16 (m, 8 H), 4.32−4.52 (m, 10 H), 4.78 (s, 2 H), 4.87 (s, 6 H), 4.93 (s, 2 H), 5.91−6.17 (m, 10 H), 6.25 (d, $J = 8.0$ Hz, 1 H), 6.30 (d, $J = 8.0$ Hz, 1 H), 6.43 (s, 1 H), 6.67 (s, 2 H), 6.74−6.80 (m, 4 H), 6.87 (s, 2 H), 6.89−6.94 (m, 6 H), 7.02−7.11 (m, 10 H), 7.24−7.31 (m, 8 H), 7.40 (d, $J = 9.0$ Hz, 4 H), 7.58 (d, $J = 6.4$ Hz, 2 H), 7.64 (d, $J = 6.4$ Hz, 2 H), 7.70 (d, $J = 6.4$ Hz, 2 H), 7.82 (d, $J = 6.4$ Hz, 2 H), 8.14 (s, 2 H), 8.16 (s, 2 H), 8.32 (s, 2 H,), 8.39 (s, 2 H), 9.09 (d, $J = 6.4$ Hz, 2 H), 9.10 (d, $J = 6.4$ Hz, 2 H), 9.25 (d, $J = 6.4$ Hz, 2 H), 9.39 (d, $J = 6.4$ Hz, 2 H).

Semidumbbell Compound 3: Compound **6** (0.072 g, 0.21 mmol) and the chloride **15** (0.20 g, 0.22 mmol) were dissolved in anhydrous DMF (10 mL) and degassed (N_2, 10 min) before NaH (0.021 g of a 60% suspension in mineral oil, 0.53 mmol) was added. The reaction mixture was stirred for 45 min at room temperature, causing the initially yellow solution to become more orange. Brine (80 mL) was added (dropwise until no more gas evolution was observed), whereupon the yellow suspension was extracted with CH_2Cl_2 (3 × 40 mL). The combined organic phase was washed with brine (2 × 100 mL) and H_2O (100 mL) before being dried ($MgSO_4$). Concentration gave a yellowish brown oil, which was subjected to column chromatography (SiO_2: CH_2Cl_2/EtOAc, 2:1). The yellow band ($R_f = 0.3$) was collected and the solvent evaporated affording a yellowish brown oil, which was repeatedly dissolved in CH_2Cl_2 (2 × 10 mL) and concentrated to give the title compound **3** (0.21 g, 81%) as a yellowish brown oil. ^1H NMR (CD_3COCD_3, 300 MHz, ppm): $\delta = 2.44$ (s, 6 H), 3.29 (s, 9 H), 3.48−3.52 (m, 6 H), 3.63−3.66 (m, 6 H), 3.78−3.83 (m, 6 H), 4.08−4.16 (m, 6 H), 4.91 (s, 2 H), 5.01 (s, 2 H), 5.05 (s, 6 H), 6.79 (s, 2 H), 6.82 (d, $J = 8.8$ Hz, 2 H), 6.87 (s, 2 H), 6.96 (d, $J = 8.4$ Hz, 6 H), 7.20 (d, $J = 8.4$ Hz, 2 H), 7.32 (d, $J = 8.8$ Hz, 2 H), 7.40 (d, $J = 8.4$ Hz, 4 H). MS (MALDI−TOF): *m/z* (%) = 1203 (100) $[M]^+$, 994 (6). $C_{60}H_{69}NO_{13}S_6$ (1204.6): calcd. C 59.82, H 5.77, N 1.16, S 15.97; found C 59.92, H 5.80, N 1.20, S 15.77.

2-[4-(Methylthio)-1,3-dithiol-2-ylidene]-5-tosyl-5*H*-1,3-dithiolo[4,5-*c*]pyrrole (19): A solution of compound **10** (0.48 g, 0.99 mmol) in anhydrous THF (70 mL) was degassed (N_2, 10 min) before a solution of CsOH·H_2O (0.18 g, 1.05 mmol) in anhydrous MeOH (8 mL) was added dropwise with a syringe over a period of 50 min at room temperature. The mixture was stirred for 15 min before MeI (1.0 mL, 2.3 g, 16 mmol) was added in one portion, whereupon the reaction mixture was stirred for 2 h and then purged with N_2 (20 min). The solvent was evaporated and the resulting yellow residue was dissolved in CH_2Cl_2 (75 mL), washed with H_2O (3 × 75 mL) and dried ($MgSO_4$). Removal of the solvent gave a yellowish orange solid, which was purified by column chromatography (SiO_2: CH_2Cl_2). The broad yellow band ($R_f = 0.6$) was collected and concentrated to give the title compound **19** (0.43 g, 98%) as a yellowish orange solid. M.p. 149−151 °C. Recrystallization from CH_2Cl_2/MeOH gave **19** as yellow crystals. M.p. 161−163 °C. ^1H NMR (CD_3SOCD_3, 300 MHz, ppm): $\delta = 2.38$ (s, 3 H), 2.43 (s, 3 H), 6.75 (s, 1 H), 7.38 (s, 2 H), 7.45 (d, $J = 8.5$ Hz, 2 H), 7.82 (d, $J = 8.5$ Hz, 2 H). ^{13}C NMR (CD_3SOCD_3, 75 MHz, ppm): $\delta =$

18.5, 21.1, 112.6 (2 signals overlapping), 114.5, 116.8, 118.8, 126.3, 126.3, 126.8, 126.9, 130.4, 134.4, 145.8. MS (EI): *m/z* (%) = 443 (54) $[M]^+$, 288 (100) $[M - Ts]^+$. $C_{16}H_{13}NO_2S_6$ (443.7): calcd. C 43.31, H 2.95, N 3.16, S 43.36; found C 43.46, H 2.95, N 3.24, S 43.49.

2-[4-(Methylthio)-1,3-dithiol-2-ylidene]-5*H*-1,3-dithiolo[4,5-*c*]pyrrole (7): Compound **19** (0.38 g, 0.86 mmol) was dissolved in anhydrous THF/MeOH (1:1 v/v, 100 mL) and degassed (N_2, 10 min) before NaOMe (30% in MeOH, 2.40 mL, 0.68 g, 12.6 mmol) was added in one portion. The yellow solution was heated under reflux for 15 min and cooled to room temperature, whereupon the solvent was evaporated. The yellow residue was dissolved in CH_2Cl_2 (75 mL), washed with H_2O (3 × 75 mL) and dried ($MgSO_4$). Concentration gave an orange oil, which was subjected to column chromatography (SiO_2: CH_2Cl_2). The yellow band (R_f = 0.6) was collected and concentrated, providing the title compound **7** (0.22 g, 88%) as a yellowish orange oil, which solidified upon standing to give a yellowish brown solid. M.p. 63.5−65 °C. ^{1}H NMR (CD_3SOCD_3, 300 MHz, ppm): δ = 2.44 (s, 3 H), 6.73 (s, 1 H), 6.79 (d, J = 2.3 Hz, 2 H), 11.11 (br. s, 1 H). ^{13}C NMR (CD_3SOCD_3, 75 MHz, ppm): δ = 18.5, 110.6 (2 signals overlapping), 111.6, 117.3, 117.30, 118.7, 118.8, 126.9. MS (EI): *m/z* (%) = 289 (100) $[M]^+$, 185 (52) 141 (47). $C_9H_7NS_5$ (289.5): calcd. C 37.34, H 2.44, N 4.84, S 55.38; found C 37.47, H 2.57, N 4.82, S 55.49.

Semidumbbell Compound 4: Compound **7** (0.035 g, 0.12 mmol) and the chloride **15** (0.10 g, 0.11 mmol) were dissolved in anhydrous DMF (5 mL) and degassed (N_2, 10 min) before NaH (0.011 g of a 60% suspension in mineral oil, 0.28 mmol) was added. The reaction mixture was stirred for 45 min at room temperature, causing the initially yellow solution to become more orange. Brine (50 mL) was added (dropwise until no more gas evolution was observed), whereupon the yellow suspension was extracted with CH_2Cl_2 (3 × 25 mL). The combined organic phase was washed with brine (3 × 75 mL) and dried ($MgSO_4$). Concentration gave a yellowish brown oil, which was subjected to column chromatography (SiO_2: CH_2Cl_2/EtOAc 2:1). The yellow band (R_f = 0.2) was collected and the solvent evaporated, affording a yellowish orange oil, which was repeatedly dissolved in CH_2Cl_2 (2 × 10 mL) and concentrated to give the title compound **4** (0.090 g, 71%) as a yellowish orange oil. ^{1}H NMR (CD_3COCD_3, 300 MHz, ppm): δ = 2.45 (s, 3 H), 3.29 (s, 9 H), 3.48−3.52 (m, 6 H), 3.63−3.67 (m, 6 H), 3.79−3.83 (m, 6 H), 4.09−4.16 (m, 6 H), 4.92 (s, 2 H), 5.01 (s, 2 H), 5.05 (s, 6 H), 6.57 (s, 1 H), 6.79 (s, 2 H), 6.83 (d, J = 8.4 Hz, 2 H), 6.88 (s, 2 H), 6.96 (d, J = 8.6 Hz, 6 H), 7.21 (d, J = 8.6 Hz, 2 H), 7.32 (d, J = 8.9 Hz, 2 H), 7.40 (d, J = 8.5 Hz, 4 H). MS (MALDI−TOF): *m/z* (%) = 1157 (100) $[M]^+$, 948 (6). $C_{59}H_{67}NO_{13}S_5$ (1158.5): calcd. C 61.17, H 5.83, N 1.21, S 13.84; found C 61.18, H 5.89, N 1.29, S 13.66.

Semidumbbell Compound 5: The iodide **12** (0.20 g, 0.22 mmol) was dissolved in anhydrous Me_2CO (10 mL) and NaSMe (0.16 g, 2.28 mmol) was added in one portion. The reaction mixture was stirred for 1.5 h at room temperature, whereupon the solvent was removed in vacuo. The yellow residue was dissolved in CH_2Cl_2 (100 mL), washed with H_2O (3 × 100 mL) and dried ($MgSO_4$). Concentration gave a colorless oil, which was subjected to column chromatography (SiO_2: CH_2Cl_2). The colorless band (R_f = 0.25) was collected and the solvent evaporated affording the title compound **5** (0.18 g, 99%) as a colorless foam. ^{1}H NMR ($CDCl_3$, 300 MHz, ppm): δ = 1.23 (t, J = 7.6 Hz, 3 H), 1.29 (s, 18 H), 2.15 (s, 3 H), 2.62 (q, J = 7.6 Hz, 2 H), 2.74 (t, J = 6.7 Hz, 2 H), 3.81 (t, J = 6.7 Hz, 2 H), 3.94−3.99 (m, 4 H), 4.03−4.07 (m, 2 H), 4.12−4.16 (m, 2 H), 4.26−4.32 (m, 4 H), 6.77−6.85 (m, 4 H), 7.03−7.10 (m, 10 H), 7.20−7.36 (m, 6 H), 7.87 (d, J = 8.5 Hz, 2 H). ^{13}C NMR ($CDCl_3$, 75 MHz, ppm): δ = 15.3, 16.1, 28.2, 31.4, 33.6, 34.3, 63.1, 67.3, 67.9, 68.0, 69.5, 70.0, 70.1, 71.0, 105.7, 105.7, 113.1, 114.6, 114.7, 124.0, 125.1 (2 signals overlapping), 126.6, 126.8, 126.8, 130.7, 131.0, 132.2, 139.8, 141.3, 144.1, 144.6, 148.3, 154.3, 154.3, 156.5. MS (MALDI−TOF): *m/z* (%) = 825 (100) $[M]^+$, 692 (11), 383 (12). $C_{54}H_{64}O_5S$ (825.2): calcd. C 78.60, H 7.82, S 3.89; found C 78.38, H 7.69, S 3.95.

Photophysical Experiments: All the measurements were performed in air-equilibrated Me_2CO, MeCN, or Me_2SO solutions. Hexafluorophosphate (PF_6^-) ions were the counterions in the case of all the cationic compounds/complexes. Absorption spectra were recorded with a Shimadzu UV-1601PC instrument and the temperature was controlled using a home-made, water-cooled thermostat. The estimated experimental errors are: 2 nm on band maxima and ±5% on the molar absorption coefficients.

Kinetic Experiments: The rate constants for the slipping on of $CBPQT^{4+}$ on the semidumbbell compound **3** were measured at different temperatures using absorption spectroscopy as the probe. Experiments were carried out by transferring a Me_2CO solution (1.41 mM) of the semidumbbell compound **3** (1.2 mL) and a Me_2CO solution (1.41 mM) of the cyclophane CBPQT·4PF_6 (1.2 mL) to two separate 3.0 mL cuvettes (optical path 1 cm), which subsequently were placed in the thermostatted cell compartment of the UV/Vis spectrophotometer and then allowed to equilibrate to a constant temperature. The two solutions were then mixed, affording an equimolar solution (0.71 mM)[45] of **3** and the slipping on of $CBPQT^{4+}$ on the semidumbbell compound **3** was followed using the MPTTF/$CBPQT^{4+}$ CT band (807 nm) as the probe. The temperature T was measured in the cuvette before and after each experiment and readings of equal to or less than ±0.1 K were obtained. The data points were collected in the early stage of the experiments where the reverse process is not yet occurring to any significant extent and subjected to a first-order analysis by plotting ln A against t, where A is the absorbance (at 807 nm) at time t. The linear relationship between ln A and t was, at each particular temperature, demonstrated by calculation of the correlation coefficient and values (Table 4) of 0.985−0.999 were obtained. The k values were obtained from the slopes of these lines, according to the relationship $\ln A = k\,t + \ln A_0$ and the estimated experimental errors are ±5%.

The estimated experimental errors are ±5% for $\Delta G^{\ddagger}$, $\Delta H^{\ddagger}$. As a result of the logarithmic nature of the plots and the fact that the $\Delta G^{\ddagger}$ values only have been calculated over an approximate 20 K wide temperature range, the error in $\Delta S^{\ddagger}$ is somewhat larger: we estimate it to be ±25% for $\Delta S^{\ddagger}$.

Determination of Binding Constants (K_a values) using the ^{1}H NMR Single-Point Method: [2]Pseudorotaxane 3⊂CBPQT·4PF_6: Mixing the colorless cyclophane CBPQT·4PF_6 and the yellow semidumbbell compound **3** in equimolar proportions in CD_3COCD_3 at 298 K produced a yellow-colored solution (1.1 mM), which slowly became green. The solution was placed in a thermostatted ^{1}H NMR spectrometer and the system was allowed to equilibrate for 1 h before the ^{1}H NMR spectrum (300 MHz) was recorded. Experiments were carried out at 298, 302, 306, 310, 314, 318, and 322 K. At all of these temperatures, slowly equilibrating complexation/decomplexation scenarios were observed, and the K_a values were determined as follows: integrals of the signals in the ^{1}H NMR spectra associated with the $^+NCH_2$ and *p*-xylylene protons in both uncomplexed and complexed $CBPQT^{4+}$ component were measured, and by knowing accurately the concentrations of the semidumbbell

compound **3** and $CBPQT^{4+}$ that were dissolved initially, the K_a values are given by the expression:

$$K_a = \frac{I_c}{I_u \left(c(\mathbf{3}) - \frac{I_c}{I_u + I_c} \cdot c(CBPQT^{4+}) \right)}$$

where I_c and I_u are the integrals of a specific proton in the complexed (c) and uncomplexed species (u), respectively, and c(**3**) and $c(CBPQT^{4+})$ are the initial molar concentrations of compound **3** and $CBPQT^{4+}$, respectively.

Determination of Binding Constants (K_a values) using the UV/Vis Dilution Method: [2]Pseudorotaxane 4⊂CBPQT·4PF$_6$: Mixing the colorless cyclophane CBPQT·4PF$_6$ and the yellow semidumbbell compound **4** in equimolar proportions in Me_2CO immediately produced a green-colored solution. Appropriate dilutions produced solutions with absolute concentrations (c) in the range of 0.1 to 0.8 mM, which subsequently were placed in the thermostatted cell compartment of the UV/Vis spectrophotometer and then allowed to equilibrate to a constant temperature, before the absorbance A was measured at 825 nm (λ_{max}). Measurements were carried out at 286.8, 291.9, 297.1, 302.1, 307.2, 311.9, and 317.0 K, where the temperature T was measured in the cuvette before and after each experiment and readings of equal to or less than ±0.1 K were obtained. This resulted in 12, 11, 11, 10, 9, 8, and 8 data points [c/A, $1/A^{1/2}$]. For each particular temperature a plot of c/A against $1/A^{1/2}$ afforded a straight line with slope a of $(1/K_a\varepsilon\, l)^{1/2}$ and a y-intercept y_0 of $1/\varepsilon\, l$, where ε is the molar extinction coefficient for the CT band of the complex and l is the optical path length, according[16] to the Equation $c/A = [(1/K_a\varepsilon\, l)^{1/2}\,(1/A^{1/2})] + 1/\varepsilon\, l$. The linear relationship between c/A and $1/A^{1/2}$ at each particular temperature was demonstrated by calculation of the correlation coefficient, and values (Table 8) of 0.998−1.000 were obtained. The K_a and ε values were obtained from the relationship $K_a = y_0/a^2$, where a and $y_0 = 1/\varepsilon\, l$ is the slope and y-intercept of the line, respectively.

[2]Pseudorotaxane 5⊂CBPQT·4PF$_6$: Mixing the colorless cyclophane CBPQT·4PF$_6$ and the colorless semidumbbell compound **5** in equimolar amounts in Me_2CO immediately produced a red-colored solution. Appropriate dilutions produced solutions with absolute concentrations (c) in the range of 0.2 to 0.9 mM, which subsequently were placed in the thermostatted cell compartment of the UV/Vis spectrophotometer and then allowed to equilibrate to a constant temperature, before the absorbance A was measured at 520 nm (λ_{max}). Measurements were carried out at 286.9, 290.3, 293.4, 296.2, 299.5, 302.4, and 305.3 K where the temperature T was measured in the cuvette before and after each experiment, and readings of equal to or less than ±0.1 K were obtained. This resulted in 9, 8, 6, 5, 5, 5, and 5 data points [c/A, $1/A^{1/2}$]. For each particular temperature a plot of c/A against $1/A^{1/2}$ afforded a straight line with slope a of $(1/K_a\varepsilon\, l)^{1/2}$ and a y-intercept y_0 of $1/\varepsilon\, l$, where ε is the molar extinction coefficient for the CT band of the complex and l is the optical path length, according[16] to the Equation $c/A = [(1/K_a\varepsilon\, l)^{1/2}\,(1/A^{1/2})] + 1/\varepsilon\, l$. The linear relationship between c/A and $1/A^{1/2}$ at each particular temperature was demonstrated by calculation of the correlation coefficient, and values (Table 9) of 0.987−0.999 were obtained. The K_a and ε values were obtained from the relationship $K_a = y_0/a^2$, where a and $y_0 = 1/\varepsilon\, l$ is the slope and y-intercept of the line, respectively.

Electrochemical Experiments: Cyclic voltammetric (CV) and differential pulse voltammetric (DPV) experiments were carried out in nitrogen-purged MeCN solutions in a classical three-electrode, single-compartment cell at room temperature. The electrochemical cell was connected to a computerized AutolabPGSTAT10 potentiostat (ECO CHEMIE BV, Utrecht, The Netherlands) controlled by the GPSE software running on a personal computer. The working electrode was a platinum disk electrode, and its surface was polished immediately prior to use. The counter electrode was a platinum wire and the reference electrode was a $Ag/AgNO_3$ electrode. 1,1-Dimethylferrocene (+0.31 V vs. SCE)[46] was present as an internal standard, and all potentials are referenced to the SCE electrode. The concentration of the examined compounds and complexes was 0.1 mM to 0.5 mM, and tetrabutylammonium hexafluorophosphate (0.1 M) was added as the supporting electrolyte. All MPTTF derivatives exhibited two pairs of reversible redox waves corresponding to two one-electron processes. The reversibility of the observed processes was established by using the criteria of (1) the separation of 60 mV between cathodic and anodic peaks, (2) the close to unity ratio of the intensities of the cathodic and anodic currents, and (3) the constancy of the peak potential on changing sweep rate in the cyclic voltammograms. The same half-wave potentials were obtained from the DPV peaks and from an average of the cathodic and anodic CV peaks, as expected for reversible processes. For irreversible processes, the potentials were estimated from the DPV peaks. The experimental errors on the potentials are estimated to be ±10 mV.

Acknowledgments

This research was funded by the Danish Natural Science Research Council (SNF, project #21-03−0317) and the Familien Hede Nielsens Fond in Denmark and by the Defense Advanced Research Projects Agency (DARPA) in the United States. Some of the compound/complex characterization were supported by the National Science Foundation under equipment grant no CHE-9974928.

[1] [1a] J.-M. Lehn, *Supramolecular Chemistry*, Wiley-VCH, Weinheim, Germany, **1995**. [1b] *Comprehensive Supramolecular Chemistry* (Eds.: J. L. Atwood, J. E. D. Davies, D. D. MacNicol, F. Vögtle, D. Reinhoudt), Pergamon, Oxford, **1996**, vol. 1−11. [1c] *Science* **2002**, *295*, 2400−2421 (Viewpoint on Supramolecular Chemistry and Self-Assembly).

[2] [2a] G. Schill, *Catenanes, Rotaxanes and Knots*, Academic Press, New York, **1971**. [2b]D. M. Walba, *Tetrahedron* **1985**, *41*, 3161−3212. [2c] C. O. Dietrich-Buchecker, J.-P. Sauvage, *Chem. Rev.* **1987**, *87*, 795−810. [2d] H. W. Gibson, H. Marand, *Adv. Mater.* **1993**, *5*, 11−21. [2e] D. B. Amabilino, J. F. Stoddart, *Chem. Rev.* **1995**, *95*, 2725−2828. [2f] R. Jäger, F. Vögtle, *Angew. Chem.* **1997**, *109*, 966−980; *Angew. Chem. Int. Ed. Engl.* **1997**, *36*, 930−944. [2g] G. A. Breault, C. A. Hunter, P. C. Mayers, *Tetrahedron* **1999**, *55*, 5265−5293. [2h] *Molecular Catenanes, Rotaxanes and Knots* (Eds.: J.-P. Sauvage, C. O. Dietrich-Buchecker), VCH-Wiley, Weinheim, **1999**. [2i] L. Raehm, D. G. Hamilton, J. K. M. Sanders, *Synlett* **2002**, 1743−1761. [2j] J. F. Stoddart, H.-R. Tseng, *Proc. Natl. Acad. Sci. USA* **2002**, *99*, 4797−4800. [2k] F. G. Gatti, S. León, J. K. Y. Wong, G. Bottari, A. Altieri, M. A. F. Morales, S. J. Teat, C. Frochot, D. A. Leigh, A. M. Brouwer, F. Zerbetto, *Proc. Natl. Acad. Sci. USA* **2003**, *100*, 10−14.

[3] [3a] M. Gómez-López, J. A. Preece, J. F. Stoddart, *Nanotechnology* **1996**, *7*, 183−192. [3b] M. D. Ward, *Chem. Ind.* **1997**, 640−645. [3c] V. Balzani, M. Gómez-López, J. F. Stoddart, *Acc. Chem. Res.* **1998**, *31*, 405−414. [3d] J.-P. Sauvage, *Acc. Chem. Res.* **1998**, *31*, 611−619. [3e] A. Niemz, V. M. Rotello, *Acc. Chem. Res.* **1999**, *32*, 42−52. [3f] A. E. Kaifer, *Acc. Chem. Res.* **1999**, *32*, 62−71. [3g] L. Fabbrizzi, M. Licchelli, P. Pallavicini, *Acc. Chem. Res.* **1999**, *32*, 846−853. [3h] D. A. Leigh, A. Murphy, *Chem. Ind.* **1999**, 178−183. [3i] M. D. Ward, *Chem. Ind.*

2000, 22−26. [3j] V. Balzani, A. Credi, F. M. Raymo, J. F. Stoddart, *Angew. Chem.* **2000**, *112*, 3486−3531; *Angew. Chem. Int. Ed.* **2000**, *39*, 3348−3391. [3k] R. Ballardini, V. Balzani, A. Credi, M. T. Gandolfi, M. Venturi, *Acc. Chem. Res.* **2001**, *34*, 445−455. [3l] A. Harada, *Acc. Chem. Res.* **2001**, *34*, 456−464. [3m] J.-P. Collin, C. Dietrich-Buchecker, P. Gavina, M. C. Jiménez-Molero, J.-P. Sauvage, *Acc. Chem. Res.* **2001**, *34*, 477−487. [3n] C. Joachim, J. K. Gimzewski, *Struct. Bonding* **2001**, *99*, 1−18. [3o] T. R. Kelly, J. P. Sestelo, *Struct. Bonding* **2001**, *99*, 19−54. [3p] J.-P. Sauvage, L. Raehm, *Struct. Bonding* **2001**, *99*, 55−78. [3q] V. Amendola, L. Fabbrizzi, C. Mangano, P. Pallavicini, *Struct. Bonding* **2001**, *99*, 79−116. [3r] M. Sano, *Struct. Bonding* **2001**, *99*, 117−140. [3s] J. Liu, M. Gómez-Kaifer, A. E. Kaifer, *Struct. Bonding* **2001**, *99*, 141−162. [3t] R. Ballardini, V. Balzani, A. Credi, M. T. Gandolfi, M. Venturi, *Struct. Bonding* **2001**, *99*, 163−188. [3u] A. R. Pease, J. F. Stoddart, *Struct. Bonding* **2001**, *99*, 189−236. [3v] A. N. Shipway, E. Katz, I. Willner, *Struct. Bonding* **2001**, *99*, 237−282. [3w] C. A. Stanier, S. J. Alderman, T. D. W. Claridge, H. L. Anderson, *Angew. Chem.* **2002**, *114*, 1847−1850; *Angew. Chem. Int. Ed.* **2002**, *41*, 1769−1772. [3x] D. A. Leigh, J. K. Y. Wong, F. Dehez, F. Zerbetto, *Nature* **2003**, *424*, 174−179. [3y] P. R. Carlier, *Angew. Chem.* **2004**, *116*, 2654−2657; *Angew. Chem. Int. Ed.* **2004**, *43*, 2602−2604. [3z] Q.-C. Wang, D.-H. Qu, J. Ren, K. C. Chen, H. Tian, *Angew. Chem.* **2004**, *116*, 2715−2719; *Angew. Chem. Int. Ed.* **2004**, *43*, 2661−2665.

[4] [4a] J. K. Gimzewski, C. Joachim, R. R. Schlittler, V. Langlais, H. Tang, I. Johannsen, *Science* **1998**, *281*, 531−533. [4b] T. R. Kelly, H. De Silva, R. A. Silva, *Nature* **1999**, *401*, 150−152. [4c] N. Koumura, R. W. J. Zijlstra, R. A. van Delden, N. Harada, B. L. Feringa, *Nature* **1999**, *401*, 152−155. [4d] T. R. Kelly, R. A. Silva, H. De Silva, S. Jasmin, Y. Zhao, *J. Am. Chem. Soc.* **2000**, *122*, 6935−6949. [4e] B. L. Feringa, R. A. van Delden, N. Koumura, E. M. Geertsema, *Chem. Rev.* **2000**, *100*, 1789−1816. [4f] C. A. Schalley, K. Beizai, F. Vögtle, *Acc. Chem. Res.* **2001**, *34*, 465−476. [4g] B. L. Feringa, *Acc. Chem. Res.* **2001**, *34*, 504−513. [4h] T. R. Kelly, *Acc. Chem. Res.* **2001**, *34*, 514−522. [4i] N. Koumura, E. M. Geertsema, M. B. van Gelder, A. Meetsma, B. L. Feringa, *J. Am. Chem. Soc.* **2002**, *124*, 5037−5051. [4j] T. Hugel, N. B. Holland, A. Cattani, L. Moroder, M. Seitz, H. E. Gaub, *Science* **2002**, *296*, 1103−1106. [4k] M. K. J. ter Wiel, R-A. van Delden, A. Meetsma, B. L. Feringa, *J. Am. Chem. Soc.* **2003**, *125*, 15076−15086. [4l] X. Zheng, M. E. Mulcahy, D. Horinek, F. Galeotti, T. F. Magnera, J. Michl, *J. Am. Chem. Soc.* **2004**, *126*, 4540−4542.

[5] V. Balzani, A. Credi, M. Venturi, *Molecular Devices and Machines − A Journey into the Nano World*, VCH-Wiley, Weinheim, **2003**.

[6] For investigations relating to [2]catenane-based, solid-state, electronically reconfigurable, switches, see: [6a] M. Asakawa, M. Higuchi, G. Mattersteig, T. Nakamura, A. R. Pease, F. M. Raymo, T. Shimizu, J. F. Stoddart, *Adv. Mater.* **2000**, *12*, 1099−1102. [6b] C. P. Collier, G. Mattersteig, E. W. Wong, Y. Lou, K. Beverly, J. Sampaio, F. M. Raymo, J. F. Stoddart, J. R. Heath, *Science* **2000**, *289*, 1172−1175. [6c] M. R. Diehl, D. W. Steuerman, H.-R. Tseng, S. A. Vignon, A. Star, P. C. Celestre, J. F. Stoddart, J. R. Heath, *ChemPhysChem.* **2003**, *4*, 1335−1339.

[7] For electronically configurable, molecular-based, logic gates, see: [7a] C. P. Collier, E. W. Wong, M. Belohradsky, F. M. Raymo, J. F. Stoddart, P. J. Kuekes, R. S. Williams, J. R. Heath, *Science* **1999**, *285*, 391−394. [7b] E. W. Wong, C. P. Collier, M. Belohradsky, F. M. Raymo, J. F. Stoddart, J. R. Heath, *J. Am. Chem. Soc.* **2000**, *122*, 5831−5840.

[8] [8a] A. R. Pease, J. O. Jeppesen, J. F. Stoddart, Y. Luo, C. P. Collier, J. R. Heath, *Acc. Chem. Res.* **2001**, *34*, 433−444. [8b] C. P. Collier, J. O. Jeppesen, Y. Luo, J. Perkins, E. W. Wong, J. R. Heath, J. F. Stoddart, *J. Am. Chem. Soc.* **2001**, *123*, 12632−12641. [8c] Y. Luo, C. P. Collier, J. O. Jeppesen, K. A. Nielsen, E. Delonno, G. Ho, J. Perkins, H.-R. Tseng, T. Yamamoto, J. F. Stoddart, J. R. Heath, *ChemPhysChem.* **2002**, *3*, 519−525. [8d] H. Yu, Y. Luo, K. Beverly, J. F. Stoddart, H.-R. Tseng, J. R. Heath, *Angew. Chem.* **2003**, *115*, 5884−5889; *Angew. Chem. Int. Ed.* **2003**, *42*, 5706−5711. [8e] H.-R. Tseng, D. Wu, N. X. Fang, X. Zhang, J. F. Stoddart, *ChemPhysChem.* **2004**, *5*, 111−116. [8f] A. H. Flood, R. J. A. Ramirez, W.-Q. deng, R. P. Muller, W. A. Goddard III, J. F. Stoddart, *Aust. J. Chem.* **2004**, *57*, 301−322. [8g] J. O. Jeppesen, C. P. Collier, J. R. Heath, Y. Luo, K. A. Nielsen, J. Perkins, J. F. Stoddart, E. Wong, *J. Phys. IV France* **2004**, *114*, 511−513. [8h] B. W. Laursen, S. Nygaard, J. O. Jeppesen, J. F. Stoddart, *Org. Lett*, **2004**, *6*, 4167−4170.

[9] [9a] H.-R. Tseng, S. A. Vignon, J. F. Stoddart, *Angew. Chem.* **2003**, *115*, 1529−1533; *Angew. Chem. Int. Ed.* **2003**, *42*, 1491−1495. [9b] H.-R. Tseng, S. A. Vignon, P. C. Celestre, J. Perkins, J. O. Jeppesen, A. Di Fabio, R. Ballardini, M. T. Gandolfi, M. Venturi, V. Balzani, J. F. Stoddart, *Chem. Eur. J.* **2004**, *10*, 155−172.

[10] [10a] P.-L. Anelli, P. R. Ashton, R. Ballardini, V. Balzani, M. T. Gandolfi, T. T. Goodnow, A. E. Kaifer, D. Philp, M. Pietraszkiewicz, L. Prodi, M. V. Reddington, A. M. Z. Slawin, N. Spencer, C. Vicent, D. J. Williams, *J. Am. Chem. Soc.* **1992**, *114*, 193−218. [10b] B. Korybut-Daszkiewicz, A. Wieckowska, R. Bilewicz, S. Domagala, K. Wozniak, *Angew. Chem.* **2004**, *116*, 1700−1704; *Angew. Chem. Int. Ed.* **2004**, *43*, 1668−1672. [10c] P. Mobian, J.-M. Kern, J.-P. Sauvage, *Angew. Chem.* **2004**, *116*, 2446−2449; *Angew. Chem. Int. Ed.* **2004**, *43*, 2392−2395.

[11] [11a] P.-L. Anelli, N. Spencer, J. F. Stoddart, *J. Am. Chem. Soc.* **1991**, *113*, 5131−5133. [11b] R. A. Bissell, E. Córdova, A. E. Kaifer, J. F. Stoddart, *Nature* **1994**, *369*, 133−137. [11c] A. Livoreil, C. O. Dietrich-Bucheker, J.-P. Sauvage, *J. Am. Chem. Soc.* **1994**, *116*, 9399−9400. [11d] P.-L. Anelli, M. Asakawa, P. R. Ashton, R. A. Bissell, G. Clavier, R. Górski, A. E. Kaifer, S. J. Langford, G. Mattersteig, S. Menzer, D. Philp, A. M. Z. Slawin, N. Spencer, J. F. Stoddart, M. S. Tolley, D. J. Williams, *Chem. Eur. J.* **1997**, *3*, 1113−1135. [11e] P. R. Ashton, R. Ballardini, V. Balzani, I. Baxter, A. Credi, M. C. T. Fyfe, M. T. Gandolfi, M. Gómez-López, M.-V. Martínez-Díaz, A. Piersanti, N. Spencer, J. F. Stoddart, M. Venturi, A. J. P. White, D. J. Williams, *J. Am. Chem. Soc.* **1998**, *120*, 11932−11942. [11f] D. A. Leigh, A. Troisi, F. Zerbetto, *Angew. Chem.* **2000**, *112*, 358−361; *Angew. Chem. Int. Ed.* **2000**, *39*, 350−353. [11g] P. R. Ashton, R. Ballardini, V. Balzani, A. Credi, R. Dress, E. Ishow, C. J. Kleverlaan, O. Kocian, J. A. Preece, N. Spencer, J. F. Stoddart, M. Venturi, S. Wagner, *Chem. Eur. J.* **2000**, *6*, 3558−3574. [11h] A. M. Brouwer, C. Frochot, F. G. Gatti, D. A. Leigh, L. Mottier, F. Paolucci, S. Roffia, G. W. H. Wurpel, *Science* **2001**, *291*, 2124−2128. [11i] A. Alteri, F. G. Gatti, E. R. Kay, D. A. Leigh, D. Martel, F. Paolucci, A. M. Z. Slawin, J. K. Y. Wong, *J. Am. Chem. Soc.* **2003**, *125*, 8644−8654. [11j] C. M. Keaveney, D. A. Leigh, *Angew. Chem.* **2004**, *116*, 1242−1244; *Angew. Chem. Int. Ed.* **2004**, *43*, 1222−1224. [11k] L. S. Jiang, J. Okano, A. Orita, J. Otera, *Angew. Chem.* **2004**, *116*, 2173−2176; *Angew. Chem. Int. Ed.* **2004**, *43*, 2121−2124.

[12] J. F. Stoddart, *Chem. Aust.* **1992**, *59*, 546−547 and 581.

[13] [13a] A. G. Kolchinski, D. H. Busch, N. W. Alcock, *J. Chem. Soc., Chem. Commun.* **1995**, 1289−1291. [13b] P. R. Ashton, P. T. Glink, J. F. Stoddart, P. A. Tasker, A. J. P. White, D. J. Williams, *Chem. Eur. J.* **1996**, *2*, 729−736. [13c] N. Solladié, J.-C. Chambron, C. O. Dietrich-Buchecker, J.-P. Sauvage, *Angew. Chem.* **1996**, *108*, 957−960; *Angew. Chem. Int. Ed. Engl.* **1996**, *35*, 906−909. [13d] P. R. Ashton, R. Ballardini, V. Balzani, M. Belohradsky, M. T. Gandolfi, D. Philp, L. Prodi, F. M. Raymo, M. V. Reddington, N. Spencer, J. F. Stoddart, M. Venturi, D. V. Williams, *J. Am. Chem. Soc.* **1996**, *118*, 4931−4951. [13e] A. P. Lyon, D. H. Macartney, *Inorg. Chem.* **1997**, *36*, 729−736. [13f] A.S. Lane, D. A. Leigh, A. Murphy, *J. Am. Chem. Soc.* **1997**, *119*, 11092−11093. [13g] S. Anderson, R. T. Aplin, T. D. W. Claridge, T. Goodson III, A. C. Maciel, G. Rumbles, J. F. Ryan, H. L. Anderson, *J. Chem. Soc., Perkin Trans. 1* **1998**,

2383−2398. [13h] A. E. Rowan, P. P. M. Aarts, K. W. M. Koutstaal, *Chem. Commun.* **1998**, 611−612. [13i] A. G. Kolchinski, N. W. Alcock, R. A. Roesner, D. H. Busch, *Chem. Commun.* **1998**, 1437−1438. [13j] S. J. Loeb, J. A. Wisner, *Chem. Commun.* **1998**, 2757−2758. [13k] G. M. Hübner, J. Gläser, C. Seel, F. Vögtle, *Angew. Chem.* **1999**, *111*, 395−398; *Angew. Chem. Int. Ed.* **1999**, *38*, 383−386. [13l] S. J. Rowan, S. J. Cantrill, J. F. Stoddart, *Org. Lett.* **1999**, *1*, 129−132. [13m] L. Raehm, J.-M. Kern, J.-P. Sauvage, *Chem. Eur. J.* **1999**, *5*, 3310−3317. [13n] C. Seel, F. Vögtle, *Chem. Eur. J.* **2000**, *6*, 21−24. [13o] S. J. Loeb, J. A. Wisner, *Chem. Commun.* **2000**, 845−846. [13p] K. Chichak, M. C. Walsh, N. R. Branda, *Chem. Commun.* **2000**, 847−848. [13q] J. E. H. Buston, J. R. Young, H. L. Anderson, *Chem. Commun.* **2000**, 905−906. [13r] S. J. Cantrill, D. A. Fulton, A. M. Heiss, A. R. Pease, J. F. Stoddart, A. J. P. White, D. J. Williams, *Chem. Eur. J.* **2000**, *6*, 2274−2287. [13s] S.-H. Chiu, J. F. Stoddart, *J. Am. Chem. Soc.* **2002**, *124*, 4174−4175. [13t] J. A. Wisner, P. D. Beer, M. G. B. Drew, M. R. Sambrook, *J. Am. Chem. Soc.* **2002**, *124*, 12469−12476. [13u] S.-H. Chiu, S. J. Rowan, S. J. Cantrill, J. F. Stoddart, A. J. P. White, D. J. Williams, *Chem. Eur. J.* **2002**, *8*, 5170−5183. [13v] R. G. E. Coumans, J. A. A. W. Elemans, P. Thordarson, R. J. M. Nolte, A. E. Rowan, *Angew. Chem.* **2003**, *115*, 674−678; *Angew. Chem. Int. Ed.* **2003**, *42*, 640−654. [13w] P. Thordarson, R. J. M. Nolte, A. E. Rowan, *Aust. J. Chem.* **2004**, *57*, 323−327. [13x] L. Hogg, D. A. Leigh, P. J. Lusby, A. Morelli, S. Parsons, J. K. Y. Wong, *Angew. Chem.* **2004**, *116*, 1238−1241; *Angew. Chem. Int. Ed.* **2004**, *43*, 1218−1221.

[14] M. C. T. Fyfe, J. F. Stoddart, *Acc. Chem. Res.* **1997**, *30*, 393−401.

[15] [15a] J. O. Jeppesen, J. Perkins, J. Becher, J. F. Stoddart, *Angew. Chem.* **2001**, *113*, 1256−1261; *Angew. Chem. Int. Ed.* **2001**, *40*, 1216−1221. [15b] J. O. Jeppesen, K. A. Nielsen, J. Perkins, S. A. Vignon, A. Di Fabio, R. Ballardini, M. T. Gandolfi, M. Venturi, V. Balzani, J. Becher, J. F. Stoddart, *Chem. Eur. J.* **2003**, *9*, 2982−3007.

[16] UV/Vis dilution experiments were carried out to determine the binding constants (K_a) for the 1:1 complexation of $CBPQT^{4+}$ with the MPTTF derivatives **6** and **7**, respectively, in Me_2CO at 298 K. The complexation of **6**/**7** by $CBPQT^{4+}$ was followed by correlating the maximum absorptions of the CT bands with the absolute concentrations of the components as described in M. B. Nielsen, J. O. Jeppesen, J. Lau, C. Lomholt, D. Damgaard, J. P. Jacobsen, J. Becher, J. F. Stoddart, *J. Org. Chem.* **2001**, *66*, 3559−3563.

[17] J. O. Jeppesen, J. Perkins, J. Becher, J. F. Stoddart, *Org. Lett.* **2000**, *2*, 3547−3550.

[18] [18a] J. O. Jeppesen, K. Takimiya, F. Jensen, J. Becher, *Org. Lett.* **1999**, *1*, 1291−1294. [18b] J. O. Jeppesen, K. Takimiya, F. Jensen, T. Brimert, K. Nielsen, N. Thorup, J. Becher, *J. Org. Chem.* **2000**, *65*, 5794−5805.

[19] C. Jia, D. Zhang, X. Guo, S. Wan, W. Xu, D. Zhu, *Synthesis* **2002**, 2177−2182.

[20] It is well established that organic reactions with a negative volume of activation ($\Delta V^{\ddagger}$) are favored by high pressure, see: F.-G. Klärner, F. Wurche, *J. Prakt. Chem.* **2000**, *342*, 609−636.

[21] [21a] D. Philp, A. M. Z. Slawin, N. Spencer, J. F. Stoddart, D. J. Williams, *J. Chem. Soc., Chem. Commun.* **1991**, 1584−1586. [21b] W. Devonport, M. A. Blower, M. R. Bryce, L. M. Goldenberg, *J. Org. Chem.* **1997**, *62*, 885−887. [21c] See: a) ref.[16]. [21d] R. Ballardini, V. Balzani, A. Di Fabio, M. T. Gandolfi, J. Becher, J. Lau, M. B. Nielsen, J. F. Stoddart, *New J. Chem.* **2001**, *25*, 293−298.

[22] [22a] P. R. Ashton, R. Ballardini, V. Balzani, S. E. Boyd, A. Credi, M. T. Gandolfi, M. Gómez-López, S. Iqbal, D. Philp, J. A. Preece, L. Prodi, H. G. Ricketts, J. F. Stoddart, M. S. Tolley, M. Venturi, A. J. P. White, D. J. Williams, *Chem. Eur. J.* **1997**, *3*, 152−170. [22b] R. Wolf, M. Asakawa, P. R. Ashton, M. Gómez-López, C. Hamers, S. Menzer, I. W. Parsons, N. Spencer, J. F. Stoddart, M. S. Tolley, D. J. Williams, *Angew. Chem.* **1998**, *110*, 1018−1022; *Angew. Chem. Int. Ed.* **1998**, *37*, 975−979. [22c] V. Balzani, A. Ceroni, A. Credi, M. Gómez-López, C. Hamers, J. F. Stoddart, R. Wolf, *New J. Chem.* **2001**, *25*, 25−31.

[23] Indeed, calculations have shown that the bis(methyleneoxy) groups are of paramount importance in assisting the $CBPQT^{4+}$ complexation process by virtue of their entering into [C−H···O] interactions with some of the α-CH hydrogen atoms in the bipyridinum units of $CBPQT^{4+}$, see: K. N. Houk, S. Menzer, S. P. Newton, F. M. Raymo, J. F. Stoddart, D. J. Williams, *J. Am. Chem. Soc.* **1999**, *121*, 1479−1487.

[24] M. Asakawa, W. Dehaen, G. L′abbé, S. Menzer, J. Nouwen, F. M. Raymo, J. F. Stoddart, D. J. Williams, *J. Org. Chem.* **1996**, *61*, 9591−9595.

[25] K. J. Laidler, *Chemical Kinetics*, Harper Collins Publisher, New York, **1987**.

[26] For further details, see the Exp. Sect.

[27] At each temperature, first-order kinetics are obeyed, i.e., good straight lines are observed (see Table 4) when ln A is plotted against t, where A is absorbance (at 807 nm) at time t. This outcome is a consequence of the fact that the data points were collected in the early stages of the experiments where the reverse process is not yet occurring to any significant extent.

[28] The $\Delta G^{\ddagger}$ values were calculated using the Eyring relationship $\Delta G^{\ddagger} = -RT\ln(kh/k_BT)$, where R is the gas constant, T is the absolute temperature, k is the rate constant, h is the Planck constant and k_B is the Boltzmann constant.

[29] The rate of complexation/decomplexation for $CBPQT^{4+}$ with the semidumbbell compound **4** was determined by coalescence of the SMe signals for the complexed and uncomplexed forms. The rate constant was calculated using the equation $k_c = (\pi v_{ex})/\sqrt{2}$, where v_{ex} was determined to be 40 Hz. At the coalescence temperature of 238 K, k_c was calculated to be 89 s^{-1}.

[30] The rate of complexation/decomplexation for $CBPQT^{4+}$ with the semidumbbell compound **5** was determined by partial line shape analysis of the $-CH_2CH_3$ signals for the complexed and complexed forms. The chemical shifts, line widths and integrations were used as input and determined from the low temperature spectrum where no exchange is observed. Simulation of the spectra using the Spinworks program (Spinworks Version 1.3, K, Marat, University of Manitoba, Department of Chemistry) gave the data reported in Table 5.

[31] J. O. Jeppesen, S. A. Vignon, J. F. Stoddart, *Chem. Eur. J.* **2003**, *9*, 4611−4625.

[32] K. A. Connors, *Binding Constants*, Wiley Interscience, New York, **1987**.

[33] An SMe group attached to an MPTTF unit reveals significant changes in its chemical shift when the MPTTF unit is located "inside" the $CBPQT^{4+}$ ring. Such an SMe group resonates at a chemical shift higher than $\delta = 2.6$ ppm, whereas an "uncomplexed" SMe group has a chemical shift of about $\delta = 2.40$ ppm. See: a) ref.[15]; b) ref.[17].

[34] At 298 K, the resonances associated with the $^{+}NCH_2$ and *p*-xylylene protons in **3**⊂$CBPQT^{4+}$ is observed at $\delta = 6.01$ and 8.06 ppm, respectively, while the $^{+}NCH_2$ and *p*-xylylene protons in the uncomplexed $CBPQT^{4+}$ resonate at $\delta = 6.09$ and 7.85 ppm, respectively.

[35] The $\Delta G°$ values were calculated using the relationship $\Delta G° = -RT\ln K_a$ where R is the gas constant and T is the absolute temperature.

[36] The K_{eq} value for the equilibrium between **2**·$GREEN^{4+}$ and **2**·RED^{4+} was calculated using the relationship $K_{eq} = \exp[(-\Delta\Delta G°)/RT)]$ where $\Delta\Delta G° = \Delta G°$(**4**⊂$CBPQT^{4+}$) − $\Delta G°$(**5**⊂$CBPQT^{4+}$), R is the gas constant and T is the absolute temperature.

[37] V. Balzani, A. Credi, G. Mattersteig, O. A. Matthews, F. M. Raymo, J. F. Stoddart, M. Venturi, A. J. P. White, D. J. Williams, *J. Org. Chem.* **2000**, *65*, 1924−1936.

[38] The distinction between rotaxanes and pseudorotaxanes is far from being a straightforward one. When size-complementarity between the stoppers and the macrocyclic component is

achieved, certain "rotaxanes" behave as pseudorotaxanes and can dissociate into their constituent components under appropriate conditions. Thus, a species which is a rotaxane at ambient temperature might well be a pseudorotaxane at elevated temperatures. Even a solvent change can turn a rotaxane into a pseudorotaxane at the same temperature. See: [38a] F. M. Raymo, J. F. Stoddart, *Chem. Rev.* **1999**, *99*, 1643−1663. [38b] S.-H. Chiu, S. J. Rowan, S. Cantrill, P. T. Glink, R. L. Garrell, J. F. Stoddart, *Org. Lett.* **2000**, *2*, 3631−3634. [38c] A. Affeld, G. M. Hübner, C. Seel, C. A. Schalley, *Eur. J. Org. Chem.* **2001**, 2877−2890. [38d] J. O. Jeppesen, J. Becher, J. F. Stoddart, *Org. Lett.* **2002**, *4*, 557−560.

[39] Several studies have shown that the complexation of $CBPQT^{4+}$ with different electron donors is at least three times stronger in MeCN than in Me_2CO, see: [39a] A. Mirzoian, A. E. Kaifer, *J. Org. Chem.* **1995**, *60*, 8093−8095. [39b] Ref.[15b]. [39c] Ref.[21c]. Assuming that the K_a value for the complexation of $CBPQT^{4+}$ with the semidumbbell compound **4** in MeCN is the same as the K_a value in Me_2CO (3950 M^{-1}), then the fraction of the [2]pseudorotaxane **4**⊂$CBPQT^{4+}$ is at least 88% in a MeCN solution containing 0.2 m M of **4** and 10 equivalents of $CBPQT^{4+}$.

[40] [40a] M. Asakawa, P. R. Ashton, V. Balzani, A. Credi, G. Mattersteig, O. A. Matthews, N. Montalti, N. Spencer, J. F. Stoddart, M. Venturi, *Chem. Eur. J.* **1997**, *3*, 1992−1996. [40b] M. Asakawa, P. R. Ashton, V. Balzani, S. E. Boyd, A. Credi, G. Mattersteig, S. Menzer, M. Montalti, F. M. Raymo, C. Ruffilli, J. F. Stoddart, M. Venturi, D. J. Williams, *Eur. J. Org. Chem.* **1999**, 985−994.

[41] The presence of folded conformations wherein the MPTTF unit enters into an "alongside" interaction with the $CBPQT^{4+}$ ring has previously been observed in both bistable [2]rotaxanes and [2]pseudorotaxanes incorporating an MPTTF unit and a DNP moiety on the rod-section of its dumbbell component, see: [41a] ref.[15b]. [41b] ref.[31]. [41c] I. C. Lee, C. W. Frank, T. Yamamoto, H.-R. Tseng, A. H. Flood, J. F. Stoddart, J. O. Jeppesen, *Langmuir* **2004**, *20*, 5809−5828.

[42] A bistable [2]rotaxane comprising two hydrophobic stoppers and incorporating TTF and DNP recognition sites in its dumbbell component and $CBPQT^{4+}$ as the ring component has very recently been reported, see: Ref.[9]. It was shown that this molecule exists almost exclusively as the translational isomer where $CBPQT^{4+}$ encircles the TTF unit. However, this translational isomer exists as a *cis*/*trans* isomeric mixture.

[43] D. D. Perrin, W. L. F. Armarego, *Purification of Laboratory Chemicals*, Pergamon Press, New York, **1988**.

[44] A. L. Van Geet, *Anal. Chem.* **1970**, *42*, 679−680.

[45] In the case of the experiments carried out at 290.5, 293.3, and 296.2 K, the initial concentration of the semi-dumbbell compound **3** and $CBPQT{\cdot}4PF_6$ was 0.93 mM.

[46] S. F. Nelsen, L.-J. Chen, M. T. Ramm, G. T. Voy, D. R. Powell, M. A. Aceola, T. R. Seehafer, J. J. Sabelko, J. R. Pladziewicz, *J. Org. Chem.* **1996**, *61*, 1405−1412.

[47] [47a] M. Feigel, H. Kessler, D. Leibfritz, *J. Am. Chem. Soc.* **1979**, *101*, 1943−1950. [47b] B. E. Mann, *J. Magn. Reson.* **1977**, *25*, 91−94.

Received July 27, 2004

